

1 [Reviewer 1 :](#)

2 **General Suggestions**

3 # Review on the paper "A nonstationary analysis for investigating the  
4 multiscale variability of extreme surges: case of the English Channel coasts"

5 ## General comments

6 In the research manuscript, the authors present an analysis of time series of  
7 storm surges in five stations along the coast of the English Channel.

8 The study is two-fold: a first part is related to the analysis of the monthly  
9 extreme storm-surges signals, by using a multi-scale wavelet analysis in order  
10 to describe the

11

12 [Answer to Reviewer 1 :](#)

13 Thank you for the different suggestions and comments useful for the  
14 improvement of the manuscript.

15 The text of **the manuscript has been checked by the authors and has been**  
16 **simplified to make easier the writing and the understanding of the different**  
17 **sections, in particular the** discussion and the methodology.

18 Also, some information has been moved from the methodological part to the  
19 results. Two illustrations related to the original hydrodynamic data (Figure 4  
20 in the new version) and the morphological defects (Figure 2 in the new  
21 version).

22 The answers will be addressed for each specific comment.

23 **[### 2. Data](#)**

24 It no very clear in the paper if storm surge or the sea level height data is used.  
25 Only the later is measured by the tide gauge, and thus a pre-processing step  
26 is required to filter out the tides and the sea-level rise. The description of this  
27 pre-processing seems to be missing in the paper. Another question is about  
28 the availability of the large-scale atmospheric circulations indices (NAO,  
29 AMO...) during the whole period covered by the tide gauges. In particular, the  
30 Brest station has measurements from 1850, so one could wonder if the indices  
31 are available from the date, and what could be the quality of such values. I  
32 think that the paper could benefit from some discussion on this point.

33 [Answer](#)

34 *Thank you for this suggestion.*

35 According to the determination of surges, a new part explaining this extraction has been  
36 added in the new version: part 3.1;

37 According to the availability of the large-scale atmospheric circulations indices (NAO,  
38 AMO...), they have been extracted from the NCEP-NCAR Reanalysis fields with the same  
39 period of the surges.

40 Timeseries of surges

41 Weymouth: 1991-2018

42 Brest: 1846-2018

43 Dunkirk:1964-2018

44 Dover: 1958-2018

45 Cherbourg: 1964-2018

46

47 Timeseries of the correlations Climate index - maximum surges

48 The correlation has been carried depending on the length of the

49

50 AMO/BREST: 1880 – 2017

51 NAO /Brest : 1865-2017

52 SLP /Brest : 1948-2017

53 ZW /Brest : 1865-2017

54

55 AMO – NAO – SLP - ZW/ Cherbourg - Dunkirk : 1964-2017

56 AMO – NAO – SLP - ZW/Douvres : 1958-2017

57 AMO – NAO – SLP- ZW/Weymouth : 1991-2017

58

59 The methodological approach has benefit from this information.

60

61

### 62 **### 3. Extreme value models**

63 The authors use the classical extreme value distribution (GEV) to model the  
64 monthly maxima of storm surges, making the distribution non-stationary by  
65 incorporating climate indices as covariates.

66 Although the presentation of the model is rather clear, the data on which the  
67 model is applied is not as clear to me: is it on the initial time series of storm  
68 surges or on the spectral components? On L200, it seems that the model is  
69 applied to each spectral component, but the justification of using a GEV  
70 distribution is then questionable since the component by itself is not extreme  
71 nor a maxima, and thus an extreme value distribution is not justified. Marginal  
72 distributions of the variable on which the GEV is fitted could give some insight  
73 on the adequacy of a GEV, in addition to the QQ plots of Figure  
74 10.

75 I have another remark about model selection: the authors do not show the  
76 fitted parameters values nor the associated confidence intervals, but only the  
77 AIC values in Table  
78 3. Such values would be necessary to address the fit and to discuss whether  
79 or not the influences of the indices are significant. The authors are only  
80 selecting the parameter that cannot be considered as stationary, but not the  
81 index that is relevant to explain the non-stationary.  
82

### 83 **Answer**

84 *The authors try to add more clarifications related to the application of the GEV*  
85 *model.*

86 *Indeed, the maxima of surges has been decomposed to different frequencies to*  
87 *which the model has been applied. This approach has been applied by Turki et*  
88 *al., 2019 ; 2020. The low and the high frequencies of the maxima highlight the*  
89 *different fluctuations of the signal and their multiscale variability. The*  
90 *prediction of each fluctuation has been investigated by the use of nonstationary*  
91 *GEV model with the incorporation of climate indices.*

92

### 93 **### 4. Multi-timescale variability of extreme surges**

94 The authors describe the results of the continuous wavelet transform (CWT)  
95 on the monthly maxima of storm surges to assess the non-stationary  
96 behavior;

### 97 **Answer**

98 *The authors have used the CWT to identify the spectrum of the extreme signal and its*  
99 *distribution in space (between station) and time (during the period of study); (Figure 2).*

100 *The authors have shown also (Fig 3) that the low frequencies ( lower than 10 year) are*  
101 *clearly observed from the CWT of the extreme surges, and less identified from the mean*  
102 *surges.*

103 *In this part, a quantification of the spectral components has been presented (Figure 4).*

104

## 105 **### 5. Large-scale climate North-Atlantic oscillations and** 106 **their link to extreme surges in the English Channel**

107

108 This section is two-fold : first, exhibit the link between the indices and the  
109 monthly maxima of storm surges and fit the GEV distribution to the  
110 components of the storm surge.

111 The authors look at the wavelet coherence to address this question and  
112 conclude that:

113 Each timescale exhibits mainly strong links with its associated climate index  
114 (L313)

115 Such a conclusion seems rather obvious to me because the indices are  
116 constructed that way and is not sufficient to my point of view to do variable  
117 selection in the GEV model of the following section before fitting the model.

118

119 Although the lengthy discussion about the visual inspection is interesting and  
120 may worth it, a proper statistical method to select the variable should be  
121 preferred.

122 Once the model is fitted, the paper falls short : since there is no variable  
123 selection and no use of the fitted model, what is the fit used for? We only can  
124 see with some difficulties the return levels of each component for the Brest  
125 station, but with little extrapolation.

126 As is, the relevance of using a GEV model is questionable.

### 127 **Answer**

128 *Thank you for these suggestions.*

129 *Indeed, according to the previous works, the effects of the climate patterns is important*  
130 *and should be considered for predicting the variability of extreme surges.*

131 *In the present research, the novel approach that an excellent prediction of the total signal*  
132 *requires a good multi-timescale prediction, i.e a prediction of each spectral component*  
133 *(provided by the MODWT analysis) which is described by an appropriate climate index ( the*  
134 *most appropriate one has been selected basing on the wavelet coherence and the monte*  
135 *carlo iterations for each component).*

136 *Indeed, the non-linear interaction between the physical mechanisms of climate patterns is*  
137 *very complex and could not considered at the same time to predict the extreme surges. To*  
138 *investigate this interaction our hypothesis consists on developing a statistical model able to*  
139 *predict the spectral component with the incorporation of the most adequate climate*  
140 *information.*

141 *The development of a full model useful for estimating the extreme surges needs the*  
142 *integration of the GEV models associated to the different timescales (~ 2-4 years; ~ 5-8 years;*  
143 *~ 12-16 years) by the means of mathematical methods; which is the objective of the further*  
144 *works. The present work bring a novel hypothesis to resolve the complex effects of climate*  
145 *patterns on the local variability of surges. This step is very important to introduce a new*  
146 *model considering the different timescales of extreme surges.*

## 147 Answer

148 *All figures have been improved in terms of quality.*

## 149 ## Technical remarks

- 150 - Spacing is not uniform in the text, please consider proof-reading;
- 151 - Parameters values are missing in Table 3;
- 152 - a "u" on L805; - Brest is missing in Figure 1; On L150:
  - 153 \*The observations which correspond to the hydrographic zero level are
  - 154 referenced to zero tide gauge (Figure 1)
  - 155 \* but seems missing;
- 156 - Figures 2-3-5-6-7-8 : the time-scales can hardly be seen, please choose
- 157 another color or another representation or another colormap.
- 158 - Figure 2 color bar is not coherent with the other Figures;
- 159 - Figures 4 and 9: the x-axis is not clear, at least 4-digit years should be
- 160 provided.
- 161 - Figure 10 a : The y-axis should be "Modeled values";
- 162 - Figure 10 b: the figure can hardly be read, please provide a larger version or
- 163 a better quality (e.g. SVG)

164

## 165 Reviewer 2 :

### 166 General Suggestions

167 The manuscript by Turki and co-authors addresses an important issue for the  
168 modeling of exceedance probability of extreme surges namely accounting for  
169 the dependence with climate patterns. The authors present an approach  
170 relying on wavelet analysis to investigate the correlation between the  
171 extreme surges and four climate oscillations (North Atlantic Oscillation, and  
172 Atlantic Multidecadal Oscillation, and the ones related to Sea-Level Pressure  
173 and Zonal Wind) at multiple time scales, \_1.5-years, \_2-4-years, and \_5-8-years  
174 and 12-16-years. On this basis, they perform nonstationary extreme value  
175 analysis using the English Channel coasts as application cases and show the  
176 added-value for accounting for these multiscale processes when deriving the  
177 return periods.

178  
179  
180  
181  
182  
183  
184  
185  
186  
187  
188  
189  
190  
191  
192  
193  
194  
195  
196  
197  
198  
199  
200  
201  
202  
203  
204  
205  
206  
207  
208  
209  
210  
211  
212  
213  
214  
215

Main comment

The manuscript is well organized and the presentation is clear. Yet, several aspects should be clarified and further elaborated before publication (state of the art, details of the implementation, discussion regarding the assumptions). Therefore, I recommend additional corrections by incorporating, if possible, the following recommendations.

## **Answer to Reviewer 2 :**

### **Specific comments**

#### **1. State of the art.**

Some key references about the link between extreme surges and climate variables should be added to the bibliography, namely:

\*\* Marcos, M., Calafat, F.M., Berihuete, Á., Dangendorf, S., 2015. Long term variations in global sea level extremes. *J. Geophys. Res.* 120(12), 8115-8134.

\*\* Marcos, M.; Woodworth, P.L., 2017. Spatiotemporal changes in extreme sea levels along the coasts of the North Atlantic and the Gulf of Mexico. *J. Geophys. Res.*, 122(9), 7031-7048.

\*\* Méndez, F. J., Menéndez, M., Luceño, A., Losada, I. J., 2007. Analyzing monthly extreme sea levels with a time-dependent GEV model. *Journal of Atmospheric and Oceanic Technology* 24(5), 894-911.

\*\* Wahl, T., Chambers, D.P., 2015. Evidence for multidecadal variability in US extreme sea level records. *J. Geophys. Res.* 120, 1527–1544.

\*\* Wahl, T.; Chambers, D.P., 2016. Climate controls multidecadal variability in US extreme sea level records. *J. Geophys. Res.* 121(2), 1274-1290.

My second concern relates to the differences of the present work with the recently published one, namely Turki et al. (2020). As far as I understood, the time scale 12- 16-years and the British part of the Channel coasts were not tackled in this published work, but it would be useful to situate in more details the present study with respect to Turki et al. (2020), for instance in the introduction.

*Thank you for the comments.*

*The proposed references have been revised and added to the state of the art.*

216 *The new funding proposed in this research, compared to the last work of Turki et al., 2020,*  
217 *has been better explained in the state of the art as suggested in line .....*

## 218 **2. Details on the implementation.**

219

220 The authors focus on extreme surges. To do so, the raw data of tide gauges  
221 should be pre-processed by accounting for the tide. Could the authors  
222 provide more details on how they proceeded? What type of tide data did  
223 they used?

224 Similarly, the authors used climate indices provided by the NCEP-NCAR  
225 Reanalysis.

226 Could the authors provide the web link where they downloaded the data for  
227 the climate indices? Besides, the authors mentioned climate oscillations  
228 using SLP and Zonal Wind. Are they directly available from NCEP-NCAR  
229 Reanalysis or are they derived from a pre-processing using EOF analysis for  
230 instance?

231 3. Model selection in the non-stationary Extreme Value Analysis (EVA).  
232 Integrating the climate drivers as covariates in EVA is a good idea, but the  
233 selection of the ‘most appropriate’ model deserves more discussion.

234

235 *Regarding the extraction of extreme surges, more details related to the classical model used*  
236 *for calculating tides are provided in the new version.*

237 *Also, the different climate indices have been better explained.*

238 *The selection of the most appropriate GEV model has been achieved for each frequency*  
239 *component. The use of the climate information has been differently explained for the*  
240 *different spectral component. For each frequency, the different climate indices have been*  
241 *tested to analyze the nonstationary behavior of the component. Then, the climate index*  
242 *associated with the best model fitting data ( i.e. showing the lowest AIC) has been selected*  
243 *and presented in this research. Similar approach has been used in Turki et al., 2020.*

244 *More explanations related to this part has been added in the new version.*

### 245 **3.1. Adequacy of GEV.**

246 It is not clear to me whether extreme value distributions are applied to each  
247 spectral component. If so, I wonder whether these variables are ‘extreme’,  
248 and whether GEV distribution is appropriate. Could the authors comment on  
249 that?

250

251 The monthly extreme surges have been calculated from hourly residual sea level. This signal  
252 has been decomposed by the MODWT to study separately the different components. Our  
253 hypothesis in the present research is the following:

254 The variability of the local extreme surges should be explained by the global climate  
255 patterns described by a series of physical mechanisms associated to the climate indices.

256 We have used the hypothesis that each spectral should be explained by a climate  
257 mechanism. Such hypothesis has been justified and validated by (1) the coherence diagrams  
258 (see also Table 2) where we have demonstrated that the effect of each climate index on the  
259 variability of extreme surges varies as a function of the spectral component and (2) the  
260 monte carlo analysis applied to each spectral component to select the most appropriate  
261 climate index. This analysis has shown a strong coherence with the first validation (1).

### 262 **3.2. Variable selection.**

263  
264 Table 2 is used to select the most appropriate climate variables to be  
265 integrated in the EVA. Though informative and useful to support discussion,  
266 my concern is that this selection is mainly based on a correlation analysis  
267 (Figure 7 and following ones), and I wonder why the authors did not perform  
268 a variable selection for the GEV model directly; for instance using AIC or  
269 selection criteria. See a discussion by Wong (2018).

270

#### 271 **Answer**

272

273 Thank you for this comment.

274 Here, a Bayesian estimation has been used to make inferences from the Likelihood function.  
275 The reason behind the choice of this approach is overcoming the limitation of short time-  
276 series with small size, the case of Weymouth station where date cover the period from 1991  
277 and 2018.

278 For each spectral component, a sample of 100.000 length has been modelled by GEV using a  
279 selected climate index. The upper and lower quantiles of the posterior probability  
280 distribution for the parameters of the MCMC sample are taken. The goodness of fit has been  
281 taken as a function of the values of the upper and the lower quantiles; best results have been  
282 considered when these values are higher than 92.5% and lower than 5.2%, respectively.

283 A new section has been added in the methodological Approach

284

#### 285 ***4 Determination of the most appropriate climate oscillation 271 connected to*** 286 ***each timescale extreme surges for GEV models***

287 Then and once selected, the most appropriate climate index has been incorporated into the  
288 GEV covariates (into the different parameters). By the use of AIC criteria, we have the best



289 results of fitting for the incorporation of this index into one (location only), two (location and  
290 scale) or three (location, scale or shape) parameters of GEV.

291 *Also, More clarifications related to this point have been added in the results (lines 573-581 of*  
292 *the new version pfd)*

293

### 294 **3.3 Model selection.**

295 Furthermore, the results for Brest in Table 3 may raise some questions:

296

297 - For scale\_12-16 years, GEV<sub>0</sub> does not seem to be the model that leads to  
298 the minimum AIC value (-1258 to be compared to -1980 for GEV<sub>1</sub>);

299

300 - For scale \_2-4-yr, the AIC values

301

302 fro GEV<sub>1-3</sub> are very close, which make very hard to identify with high  
303 confidence the most appropriate model. The authors should comment on  
304 that.

305 See also Burnham and Anderson (2004) for further details.

306 Reference:

307 Wong, T. E. (2018). An integration and assessment of multiple covariates of  
308 nonstationary storm surge statistical behavior by Bayesian model averaging.  
309 Advances in Statistical Climatology, Meteorology and Oceanography, 4(1/2),  
310 53-63.

311

312 Burnham, K. P. and Anderson, D. R.: Multimodel inference: understanding AIC  
313 and BIC in model selection, Sociolog. Meth. Res., 60, 261–304, 2004.

314

315 *It's a very interesting comment which needs more clarifications from the authors.*

316 *More discussion related to this part has been added basing on the references provided.*

317 *Also, the different results presented here still preliminary and represent a first step for*  
318 *investigating the nonstationary behavior of the different frequencies. Preliminary results*  
319 *have shown that the nonstationary behavior is mainly controlled by the high frequencies.*

320

### 321 **4. Correlation.**

322 The authors analyze the significance of the correlation through a visual  
323 inspection of the results provided by wavelet spectral analysis. In lines 339-  
324 341, the authors mentioned that they are using a Monte-Carlo-based  
325 approach to identify the most statistically significant correlation: could the  
326 authors provide more details on the implementation.

327 Is it a bootstrap-based approach? How do they analyse the changes of the

328 correlation at the Monte-Carlo iterations? Could the authors provide  
329 additional results about this significance assessment?

330 **Answer**

331 *As suggested in the previous document, a bootstrap approach has been applied to assess the*  
332 *statistical significance of the correlation between the spectral component of the extreme*  
333 *surges and the climate oscillation at each timescale. By resampling the timeseries 10.000*  
334 *times, 95% confidence intervals have been considered to extract the best climate information*  
335 *fitting the extreme surges (Villarini et al., 2009).*

336 *Here, the confidence intervals (CI) have been calculated by the bootstrap technique by*  
337 *simulating the monthly maxima of surges (spectral component) from the climate index*  
338 *(spectral component) at each timescale (new samples with a size of 1000).*

339 *When the original surges have been fitted to the simulated ones, 95% confidence intervals for*  
340 *the maximum likelihood estimates have been calculated.*

341 *A table providing the 95% CI for each spectral component and each station is added (Table 3).*

342

343

344

345

346

347

348

349

350

351

352

353

354

355

356  
357  
358  
359

*Table 3 Analysis of the statistical significance of the correlation between the spectral component of the extreme surges and the climate oscillation at each timescale for the different stations. The 95% Confidence Intervals from Bootstrap technique in Square Brackets. The most significant correlations are illustrated by the grey columns.*

360  
361

---

	<b>~ 1.5-yr</b>	<b>SLP</b>	<b>ZW</b>	<b>NAO</b>	<b>AMO</b>
	<b>Brest</b>	[0.152, 0.174]	[0.145, 0.182]	[0.141, 0.178]	[0.138, 0.189]
	<b>Cherbourg</b>	[0.161, 0.170]	[0.142, 0.179]	[0.142, 0.179]	[0.135, 0.180]
	<b>Dunkirk</b>	[0.160, 0.168]	[0.150, 0.185]	[0.150, 0.185]	[0.135, 0.183]
	<b>Dover</b>	[0.158, 0.165]	[0.161, 0.180]	[0.161, 0.180]	[0.133, 0.180]
362	<b>Weymouth</b>	[0.421, 0.429]	[0.411, 0.450]	[0.381, 0.299]	[0.375, 0.281]
	<b>~ 2-4-yr</b>				
	<b>Brest</b>	[0.145, 0.164]	[0.149, 0.158]	[0.141, 0.179]	[0.138, 0.183]
	<b>Cherbourg</b>	[0.160, 0.175]	[0.188, 0.196]	[0.161, 0.179]	[0.158, 0.182]
	<b>Dunkirk</b>	[0.145, 0.158]	[0.180, 0.185]	[0.145, 0.164]	[0.140, 0.169]
	<b>Dover</b>	[0.148, 0.163]	[0.192, 0.198]	[0.145, 0.168]	[0.143, 0.175]
363	<b>Weymouth</b>	[0.412, 0.420]	[0.420, 0.430]	[0.410, 0.425]	[0.410, 0.428]
	<b>~ 5-8-yr</b>				
	<b>Brest</b>	[0.075, 0.090]	[0.073, 0.092]	[0.085, 0.089]	[0.070, 0.096]
	<b>Cherbourg</b>	[0.190, 0.198]	[0.185, 0.198]	[0.191, 0.196]	[0.181, 0.198]
	<b>Dunkirk</b>	[0.180, 0.188]	[0.177, 0.185]	[0.183, 0.187]	[0.175, 0.187]
	<b>Dover</b>	[0.180, 0.195]	[0.180, 0.198]	[0.180, 0.184]	[0.176, 0.199]
364	<b>Weymouth</b>	[0.219, 0.222]	[0.218, 0.225]	[0.221, 0.226]	[0.216, 0.226]
365					
	<b>~ 12-16-yr</b>				
	<b>Brest</b>	[0.033, 0.046]	[0.034, 0.045]	[0.035, 0.045]	[0.038, 0.041]
	<b>Cherbourg</b>	[0.089, 0.099]	[0.090, 0.099]	[0.090, 0.097]	[0.091, 0.095]
	<b>Dunkirk</b>	[0.087, 0.099]	[0.089, 0.098]	[0.090, 0.097]	[0.093, 0.096]
	<b>Dover</b>	[0.078, 0.089]	[0.080, 0.088]	[0.080, 0.086]	[0.082, 0.085]
	<b>Weymouth</b>	[0.250, 0.260]	[0.250, 0.259]	[0.250, 0.257]	

---

366  
367  
368  
369

370 **Model for each Spectral component?**

371

372 The objective of this decomposition and the use of GEV par component.

373 The full model for estimating the extreme surges can be the sum of the  
374 different components?

375

376 **Answer**

377

378 *In any part of the manuscript, the authors have proposed the sum of the different GEV models  
379 to obtain the full model able to estimate the total signal of monthly extreme surges.*

380 *Indeed, this question remains unresolved until now. Once the model identified, how can we  
381 use them to define a stochastic tool for estimating the extreme surges?*

382 *However, this finding confirms our first hypotheses related to the connection between the  
383 most appropriate climate index and the extreme surges at each time scale. It provides also a  
384 guidance on incorporating nonstationary processes of large-scale oscillations to different  
385 spectral components informed by the wavelet techniques, the Bayesian approaches and the  
386 GEV model probabilities.*

387 *A new paragraph explaining this point has been added as a discussion part.*

388 **This study has expanded the previous works of Turki et al. (2019; 2020) upon a new approach  
389 combining spectral and probabilistic methods to integrate multiple streams of information  
390 related to climate teleconnections. Indeed, each timescale has been simulated separately with  
391 the nonstationary GEV models and expressed as a function of the most suitable climate index  
392 improving its fitting. The estimation of the total signal of surges should be determined by  
393 combining the developed nonstationary GEV models used for the different timescales.**

394 **These results should support the hypothesis introduced at the beginning of the present work  
395 suggesting that: (i) the extreme surges should depend on different timescales; (ii) each  
396 timescale should be related to a specific large-scale oscillation.**

397 **The finding is in agreement with the previous works of Lee et al. (2017) and Wang et al. (2018)  
398 highlighting the importance of a careful consideration when complex physical mechanisms of  
399 different climate indices are included into model structures for estimating extreme surges.**

400 Indeed, this work provides a guidance on incorporating nonstationary processes of large-scale  
401 oscillations to different spectral components informed by the wavelet techniques, the Bayesian  
402 approaches and the GEV model probabilities.

403 The primary contribution of the present research is to present a new approach for: (1)  
404 investigating the multi-timescale variability of the nonstationary extreme surges; (2)  
405 identifying their multi-connection with climate oscillations according to the timescale and (3)  
406 resolve in part the problems of uncertainty of most appropriate climate to use as covariate for  
407 GEV models at each timescale. However, additional models (e.g. significance tests and  
408 sensitivity analyses and modelling uncertainties) and application sites (e.g. Mediterranean and  
409 pacific ones controlled by other climate oscillations) are required to expand the developed  
410 approach.

411 Also, generating a final robust stochastic model useful for projecting storm surge return levels  
412 and assessing the flood risk management requires further efforts to build on the potentially  
413 advantageous approach presented here by integrating the GEV models associated with the  
414 different timescales through the use of mathematical methods.

415

416

417 [Figures for comparing the return levels.](#)

418 **Answer**

419 *Here, the stochastic modelling provides us some insights into the nonstationary behavior of*  
420 *extremes in relation with the climate oscillations.*

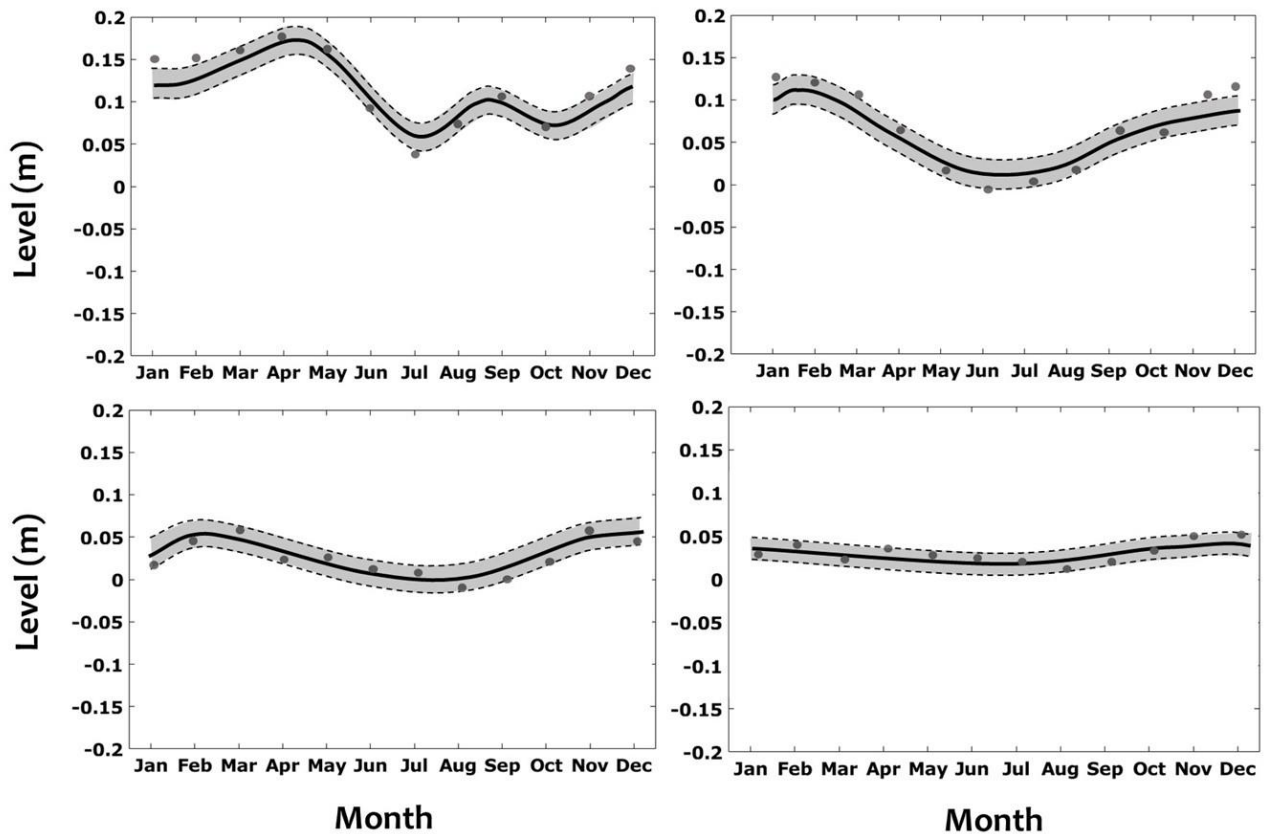
421 *The comparison between the simulated surges, using the nonstationary GEV models, and the*  
422 *original data has been illustrated in Fig.10 for Brest.*

423 *The fifty-year return level plot for the different spectral components is presented in Fig.10 c.*

424

425

426



427

428

429 *Figure 10.c Fifty-year return level of monthly values using the original data (grey circles) and*  
 430 *the best nonstationary GEV model for Brest (solid black line) at each timescale (spectral*  
 431 *component). The lower and the upper limits of the 95% confidence interval calculated using*  
 432 *the delta method (dashed black line). The associated confidence area is plotted with grey*  
 433 *shaded area.*

434

435

436

437 **5. Typo.**

438 Line 70: “investigates” should be “investigate” Line 467: “covariable” should  
 439 be covariate

440 *All typos have been checked and corrected.*

441

442

443

444

445

446 **A nonstationary analysis for investigating the multiscale**  
447 **variability of extreme surges: case of the English Channel coasts**

448  
449 Imen Turki<sup>1</sup>, Lisa Baulon<sup>1,2</sup>, Nicolas Massei<sup>1</sup>, Benoit Laignel<sup>1</sup>, Stéphane Costa<sup>3</sup>,  
450 Matthieu Fournier<sup>1</sup>, Olivier Maquaire<sup>3</sup>

451  
452 <sup>1</sup> UMR CNRS 6143 Continental and Coastal Morphodynamics 'M2C' University of Rouen,  
453 76821 Mont-Saint-Aignan Cedex, France.

454 <sup>2</sup> French Geological Survey, 3 avenue Claude Guillemin, 45060 Orléans Cedex, France

455 <sup>3</sup>UMR CNRS 6554 GEOPEN

456 Corresponding author: Imen Turki ([imen.turki@univ-rouen.fr](mailto:imen.turki@univ-rouen.fr))  
457

458 **Abstract**

459 This research examines the nonstationary dynamics of extreme surges along the English  
460 Channel coasts and seeks to make their connection to the climate patterns at different time-  
461 scales by the use of a detailed spectral analysis in order to gain insights on the physical  
462 mechanisms relating the global atmospheric circulation to the local-scale variability of the  
463 monthly extreme surges. This variability highlights different oscillatory components from the  
464 interannual (~1.5-years, ~2-4-years, ~5-8-years) to the interdecadal (~12-16-years) scales with  
465 mean explained variances of ~ 25 - 32 % and ~ 2 - 4 % of the total variability, respectively.  
466 Using the two hypotheses that the physical mechanisms of the atmospheric circulation change  
467 according to the timescales and their connection with the local variability improves the  
468 prediction of the extremes, we have demonstrated statistically significant relationships of ~1.5-  
469 years, ~2-4-years, and ~5-8-years and 12-16-years with the different climate oscillations of  
470 Sea-Level Pressure, Zonal Wind, North Atlantic Oscillation and Atlantic Multidecadal  
471 Oscillation, respectively.

472 Such physical links have been used to implement the parameters of the time-dependent GEV  
473 distribution models. The introduced climate information in the GEV parameters has  
474 considerably improved the prediction of the different time-scales of surges with an explained  
475 variance higher than 60%. This improvement exhibits their nonlinear relationship with the  
476 large-scale atmospheric circulation.

477 **Key-Words:** Coastal extreme surges, multi-timescale variability, climate oscillations,  
478 nonstationary GEV models

## 479 **1. Introduction**

480 Risks assessments has been recognized as an urgent task essential to take effective reduction  
481 of disasters and adaptation actions of climate change. The increase in coastal flood risk is  
482 generally driven by the extreme surges being the result of episodic water fluctuations due to  
483 waves and storm surges. High surges are considered as significant hazards for many low-lying  
484 coastal communities (e.g. Hanson et al., 2011; Nicholls et al., 2011) and are expected to be  
485 intensified with rising global mean sea level (Menendez and Woodworth, 2010).

486 Being an alarming problem for the coastal vulnerability, extreme events have gained the  
487 attention of the scientists who have reported the dynamics (e.g. Haigh et al., 2010; Idier et al.,  
488 2012; Masina and Lamberti, 2013; Tomasin and Pirazzoli, 2008; Turki et al., 2020) and the  
489 projections (e.g. vousdoukas et al., 2017) of extreme surges considering the stationary and the  
490 nonstationary contributions from tides, waves, sea-level-rise components (e.g. Brown et al.,



491 2010; Idier et al., 2017), and large-scale climate oscillations (e.g. Colberg et al., 2019; Turki et  
492 al., 2019; 2020).

493 Under the assumption of a stationary surges, the concepts of return level and return period  
494 provide critical information for infrastructure design, decision-making, and assessing the  
495 impacts of rare weather and climatic events (Rosbjerg and Madsen, 1998). However, the  
496 frequency of extremes has been changing and is likely to continue changing in the future (e.g.  
497 Milly et al., 2008). Therefore, concepts and models that can account for nonstationary analysis  
498 of climatic and hydrologic extremes are needed (e.g. Cooley, 2013; Salas and Obeysekera,  
499 2013; Parey et al., 2010).

500 Over the last decade, several studies adopted the nonstationary behaviour of extremes to  
501 estimate their evolution and their return-periods from rigorous models of Extreme Value  
502 Theory (EVT) by incorporating an information related to climate oscillations.

503 In this way, the recurrence of coastal extreme events over the Northern European continent and  
504 the persistence of high energetic conditions around the Atlantic have been associated with the  
505 deepening of Icelandic Low and the extension/reinforcement of the Azores High. Those facts  
506 can be interpreted, at quasi daily timescale, as the preferred excitation of a given atmospheric  
507 regime close to the positive phase of the North Atlantic Oscillation. The recent predominance

508 of this regime can be explained partly by the impact of the North Tropical Atlantic Ocean upon  
509 the midlatitude atmosphere and by the increase of greenhouse gas concentration induced by  
510 human activities.

511 Menendez and Woodworth (2010) have used a nonstationary extreme values analysis together  
512 with the NAO (North Atlantic Oscillation) and Arctic Oscillation (AO) indices for improving  
513 the estimation of monthly extreme sea-levels along the European coasts.

514 In the Northern Adriatic region, Masina et al. (2013) investigate changes in extreme sea levels  
515 applying a nonstationary approach to the monthly maxima and the climate oscillations of NAO  
516 and AO (Arctic Oscillation) indices. They have suggested that the increase in the extreme water  
517 levels since the 1990s is related to the changes in the wind regime and the intensification of  
518 Bora and Sirocco winds after the second half of the 20th century.

519 [Then, Marcos et al. \(2015\) have investigated the decadal and multidecadal changes in sea level](#)  
520 [extremes using long tide gauge records distributed worldwide. They have demonstrated that](#)  
521 [the intensity and the occurrence of the extreme sea levels vary on decadal scales in the most of](#)  
522 [the sites in relation with a common large-scale forcing. In the same way, the study of extreme](#)  
523 [sea levels along the coastal zones of the North Atlantic Ocean and the Gulf of Mexico has](#)  
524 [shown that the mean sea level should be considered as the major driver of extremes \(Marcos](#)

525 and Woodworth 2017) since the intensity of extreme episodes increases at centennial time  
526 scales, together with multidecadal variability. The extreme sea levels along the United States  
527 coastline between 1929 and 2013 have been investigated by Wahls and Chambers (2015;  
528 2016). Wahls and Chambers (2015) have identified the relation between the multidecadal  
529 variations in extreme sea and the changes in mean sea level. Such relation has been mainly  
530 pointed toward some regions where storm surges are primarily driven by extratropical cyclones  
531 and should contribute in the variation of relevant return water levels required for coastal design.  
532 Such extremes have been then investigated in Wahls and Chambers (2016) works aiming to  
533 define their relationship with the large-scale climate variability by the use of simple and  
534 multiple linear regression models.

535

536 In the English Channel, the extreme sea levels have been addressed by several works (e.g.  
537 Haigh et al., 2010; Idier et al., 2012; Tomasin and Pirazzoli, 2008; Turki et al., 2015a; Turki et  
538 al., 2019) with the aim of investigating their dynamics at different timescales and their  
539 connections to the atmospheric circulation patterns.

540 Haigh et al. (2010) investigated the interannual and the interdecadal extreme surges in the  
541 English Channel and their strong relationship with the NAO index. Their results showed weak

542 negative correlations throughout the Channel and strong positive correlations at the boundary  
543 along the Southern North Sea. Using a numerical approach, Idier et al. (2012) studied the spatial  
544 evolution of some historical storms in the Atlantic Sea and their dependence on tides.

545 Recently, Turki et al. (2019) have examined the multiscale variability of the sea-level changes  
546 in the Seine bay (NW France) in relation with the global climate oscillations from the SLP  
547 composites; they have demonstrated dipolar patterns of high-low pressures suggesting positive  
548 and negative anomalies at the interdecadal and the interannual scales respectively.

549 Despite these important advances, no particular studies exist on sea-level dynamics and  
550 extreme events linked to the large-scale climate oscillations along the English Channel  
551 coastlines. The aforementioned works of Turki et al. (2015a, 2019) have focused on the  
552 multiscale sea-level variability along the French coasts related to the NAO and the Sea-Level  
553 Pressure (SLP) patterns; however, they have not addressed the regional behaviour of the  
554 extreme sea levels in relation with the global climate oscillations.

555 Then, similar approaches have been used by Turki et al. (2020) to quantify the nonstationary  
556 behaviour of extreme surges and their relationship with the global atmospheric circulation at  
557 different timescales along the English Channel coasts (NW France) between 1964 and 2012.  
558 They have reported that the intermonthly and the interannual variability of monthly extrema

559 are statistically modelled by nonstationary GEV distribution using the full information related  
560 to the climate teleconnections.

561 In the same context, the present contribution aims to investigate the interannual and the  
562 interdecadal dynamics of extreme surges along the English Channel coasts (NW France and  
563 SW England) by the use of combining techniques of spectral analyses and probabilistic models.  
564 We hypothesize that different large-scale climate variables may be involved in explaining the  
565 occurrence of extreme surges, and that this dependence can be a function of each timescale.  
566 The rationale behind this hypothesis is based on the following: (1) each timeseries of extreme  
567 surges should depend on different timescales; (2) each timescale should be related to a specific  
568 large-scale oscillation. Using this hypothesis, the linkages between the local extreme surges  
569 and the large-scale climate oscillations are deciphered with the aim to improve the extreme  
570 models using the most consistent large-scale oscillations as covariates.

571

572 The overall approach for testing our hypotheses can be described as follows, for a given  
573 extreme surge timeseries: i) identify the short to long timescale oscillations characterizing the  
574 local variability of the extreme surges; ii) explore the correlation between the local extreme  
575 surges and the selected large-scale variable from short to long timescales; iii) select the most

576 appropriate large-scale variable as an explanatory parameter to be used as a covariate in  
577 nonstationary GEV models and estimate the extreme surges.

578 The paper is structured as follows. The used hydro-climatic data are presented in section 2,  
579 including local extreme surges and large-scale variables. Section 3 explains the methodological  
580 approach used. Finally, the sections 4 and 5 report the results related to the multiscale  
581 variability of extreme surges along the English Channel and their teleconnections with the  
582 large-scale climate oscillations required for their estimation by the use of GEV extreme models.  
583 The concluding remarks of these findings are addressed in section 6.

584

## 585 **2. Database description**

586 The present research focuses on the dynamics of extreme surges along the English Channel  
587 coasts (French and the Britannic coasts); It has been conducted in the framework of some  
588 French research programs: RICOCHET (ANR program), RAIV COT (Normandy Region  
589 program) and the international project COTEST (CNES-TOSA program) related to the future  
590 mission Surface Water and Ocean Topography (SWOT).

591 The English Channel (Figure 1) is a shallow sea between Northern France and South England,  
592 connecting Atlantic Ocean to North Sea. Melting of retreating glaciers formed a megaflood in  
593 the southern North Sea and it geographically separated Britain from Europe and formed English

594 Channel at the last Quaternary Period (Collier et al. 2015). English Channel has a complex sea  
595 floor due to its characteristics of formation. It is deep and wide on the western side, narrower  
596 and shallower towards Strait of Dover. Largest width of the Channel is around 160 km (Figure  
597 1). The average depth of the channel is about 120 m. It gradually narrows eastward to a width  
598 of 35 km and depth of around 45 m in the Dover Strait. The east to west extent of the Channel  
599 is about 500 km. The overall width of shallow depths is wider in the French side of the channel.  
600 The extreme storm surges of this area are mostly occurred by low pressure systems from the  
601 Atlantic Ocean, propagating eastwards or storm surges propagating south from the North Sea  
602 (Law, 1975). The area is exposed to major storms from Atlantic side of the channel, having a  
603 maximum fetch of winds, from west to southeast then to northwest.  
604 Three tide gauge sites along the French coasts have been used in the present study: (1) Dunkirk  
605 station which is a few kilometres away from Belgian borders, (2) Cherbourg station located on  
606 the Cotentin Peninsula and at the opening of the Atlantic Sea, (3) Brest station which is a  
607 sheltered bay located at the western extremity of metropolitan France and connected to the  
608 Atlantic Ocean.

609 Two tide gauge sites along the Britannic coasts have been used: (1) Dover station which is  
610 separated from Dunkirk by the North Sea and (2) Weymouth station symmetrically with  
611 respect to Cherbourg.

612 The French tide gauges are operated and maintained by the National French Center of  
613 Oceanographic Data (SHOM) while the Britannic tide gauges are operated by the British  
614 Oceanographic Data Center. All stations are referenced to the hydrographic zero level; they  
615 provide time-series of hourly observations measurements until 2018.

616 Available data are summarized as the following: Brest (168 years between 1850 and 2018);  
617 Cherbourg and Dunkirk (54 years between 1964 and 2018); Dover (53 years between 1963 and  
618 2018); Weymouth (28 years between 1990 and 2018).

619 The hourly measurements suffer from some gaps of daily length distributed along the time-  
620 series. These gaps have been processed by the hybrid model for filling gaps developed by Turki  
621 et al. (2015b) by using the SLP as covariate in ARMA methods and the memory effects of the  
622 previous distribution of surges to estimate the missing values and fill the gaps. This model has  
623 been used in the recent works of Turki et al., (2019; 2020).

624 The large-scale atmospheric circulations are represented in this work by four different climate  
625 indices which are considered as fundamental drivers in the Atlantic regions (Massei et al.,



626 2017; Turki et al., 2019; 2020): the Atlantic Multidecadal Oscillation (AMO), the North  
627 Atlantic Oscillation (NAO), the Zonal Wind (ZW) component extracted at 850hPa, and the  
628 Sea-Level Pressure (SLP).

629 Monthly time-series of climate indices have been provided by the NCEP-NCAR Reanalysis  
630 fields (<http://www.esrl.noaa.gov/psd/data/gridded/data.ncep.reanalysis.derived.html>) until  
631 2017. The different indices have been extracted during the same period of the sea-level  
632 observations at the four stations Cherbourg, Dunkirk, Dover and Weymouth. For the longest  
633 timeseries of Brest (1850 - 2018), the use of climate indices has been limited according to their  
634 initial date availability (AMO: 1880 – 2017; NAO: 1865-2017; SLP: 1948-2017; ZW: 1865-  
635 2017).

636

### 637 **3. Methodological Approach**

#### 638 **2. 1 Extraction of residual sea level: ‘surges’**

639

640 The total sea-level height, resulting from the astronomical and the meteorological processes,  
641 exhibits a temporal non-stationarity which is explained by a combination of the effects of the  
642 long-term trends in the mean sea level, the modulation by the deterministic tidal component  
643 and the stochastic signal of surges, and the interactions between tides and surges. The  
644 occurrence of extreme sea levels is controlled by periods of high astronomically generated  
645 tides, in particular at inter-annual scales when two phenomena of precession cause systematic  
646 variation of high tides. The modulation of the tides contributes to the enhanced risk of coastal

647 flooding. Therefore, the separation between tidal and non-tidal signals is an important task in  
648 any analysis of sea-level time-series. By the hypothesis of independence between the  
649 astronomical tides and the stochastic residual of surges, the nonlinear relationship between the  
650 tidal modulation and surges is not considered in the present analysis. Using the classical  
651 harmonic analysis, the tidal component has been modelled as the sum of a finite set of sinusoids  
652 at specific frequencies to determine the determinist phase/ amplitude of each sinusoid and  
653 predict the astronomical component of tides. In order to obtain a quantitative assessment of the  
654 non-tidal contribution in storminess changes, technical methods based on MATLAB t-tide  
655 package have been applied to the seal level measurements, demodulated from long-term  
656 components (e.g. mean sea level, vertical local movement ), for estimating year-by-year tidal  
657 constituents. A year-by-year tidal simulation (Shaw and Tsimplis, 2010) has been applied to  
658 the sea-level time-series to determine the amplitude and the phase of tidal modulations using  
659 harmonic analysis fitted to 18.61-, 9.305-, 8.85-, and 4.425-year sinusoidal signals (Pugh,  
660 1987). The radiational components have been also considered for the extraction of the  
661 stochastic component of surges (Williams et al., 2018).

### 662 ***3.2 Wavelet spectral analysis***

663 The Continuous Wavelet Transform CWT is generally used for data analysis in hydrology,  
664 geophysics, and environmental sciences (Labat, 2005; Sang, 2013; Torrence and Compo,  
665 1998). This technique produces the timescale with the means of the Fourier transform contour  
666 diagram on which the time is indicated on the x-axis, the timescale (period,) on the y-axis, and  
667 the variance (power) on the z-axis.

668 Then, a wavelet multiresolution analysis has been used to decompose the signal of monthly  
669 extreme surges into different internal components corresponding to different timescales. This  
670 decomposition consists on applying a series of iterative filtering to the signal by the use of low-  
671 pass and high-pass filters able to produce the spectral components describing the total signal.  
672 More details are presented in the recent works of Massei et al. (2017) and Turki et al., (2019).  
673 In summary, the total signal has been separated into a relatively small number of wavelet  
674 components from high to low frequencies that altogether explains the variability of the signal;  
675 this will be illustrated later using the hourly measurements and the monthly maxima of surges.

676 [The wavelet coherence has been calculated to investigate the relationship between the extreme](#)  
677 [surges and the climate oscillations by identifying the timescales where the two timeseries co-](#)  
678 [vary, even if they do not display high power. Here, a significance test has been implemented](#)  
679 [by the use of a Monte Carlo analysis based on an autocorrelation function of two timeseries \(](#)  
680 [Grinsted et al., 2004\).](#)

681

682

### 683 ***3. 3 Stationary and Nonstationary extreme value model***

684 Finally, and with the aim of addressing the nonstationary behaviour of extreme surges, the  
685 monthly maxima of the surges have been calculated and decomposed with the multiresolution  
686 analysis. Then, a nonstationary extreme value analysis based on the GEV distribution with

687 time-dependent parameters (Coles, 2001) has been implemented to model the series of the  
688 monthly maxima surges. There are several GEV families which depend on the shape parameter,  
689 e.g. Weibull ( $\varepsilon < 0$ ), Gumbel ( $\varepsilon = 0$ ), and Fréchet ( $\varepsilon > 0$ ). The three parameters of the GEV (i.e.  
690 location  $\mu$ , scale  $\psi$ , shape  $\varepsilon$ ) are estimated by the maximum likelihood function.

691 The nonstationary effect was considered by incorporating the selected climate indices (NAO,  
692 AMO, ZW, and SLP) into the parametrization of the GEV models. Akaike Information  
693 Criterion (AIC) has been used to select the most appropriate probability function models. The  
694 methods of maximum likelihood were used for the estimation of the distribution's parameters.  
695 The approach used considers the location ( $\mu$ ), the scale ( $\psi$ ), and the shape ( $\varepsilon$ ) parameters with  
696 relevant covariates, which are described by a selected climate index:

$$697 \quad \mu(t) = \beta_{0,\mu} + \beta_{1,\mu}Y_1 + \dots + \beta_{n,\mu}Y_n \quad (1)$$

$$698 \quad \psi(t) = \beta_{0,\psi} + \beta_{1,\psi}Y_1 + \dots + \beta_{n,\psi}Y_n \quad (2)$$

$$699 \quad \varepsilon(t) = \beta_{0,\varepsilon} + \beta_{1,\varepsilon}Y_1 + \dots + \beta_{n,\varepsilon}Y_n \quad (3)$$

700 Where  $\beta_0, \beta_1, \dots, \beta_n$  are the coefficients, and  $Y_i$  is the covariate represented by the climate  
701 index. For each spectral component, only one climate index can be used to be introduced into  
702 the parameters  $\mu$ ,  $\psi$ , and  $\varepsilon$  of the nonstationary GEV model (into one of them, into two of them  
703 or into the three parameters).

704 With the aim of optimizing the best use of the most appropriate climate index (detailed in  
705 section 3.4) into the different GEV parameters, a series of sensitivity analyses were  
706 implemented for each timescale. The AIC measures the goodness of the fitting of the model  
707 (Akaike, 1973) to the relation  $AIC = -2l + 2K$ ; where  $l$  is the log-likelihood value estimated for  
708 the fitted model, and  $K$  is the number of the model parameters. Higher ranked models should  
709 result from lower AIC scores.

710 The non-stationary return levels and return-periods have been calculated using Bayesian  
711 inference, implemented in the Non-stationary Extreme Value Analysis (NEVA) software R-  
712 package. The Confidence intervals for the return level estimates have been calculated by the  
713 use of the method of delta (Coles, 2001).

714

715 *3. 4 Determination of the most appropriate climate oscillation*  
716 *connected to each timescale extreme surges for GEV models*

717

718 As suggested previously, the main hypothesis presented in this research is that effects of the  
719 physical mechanisms on the extreme surges vary according to the timescale and each scale  
720 should be related to a given climate oscillation.

721 This hypothesis has been investigated by two approaches:

722 (1) a spectral approach based on the use of wavelet techniques (wavelet multiresolution and  
723 wavelet coherence as detailed in section 3.2) for optimizing the physical relationship between  
724 the climate index and the extreme surges at each timescale. Here, a bootstrap approach has  
725 been applied to assess the statistical significance of the correlation between the spectral

726 component of the extreme surges and the climate oscillation at each timescale. By resampling  
727 the timeseries 10.000 times, 95% confidence intervals have been considered to extract the best  
728 climate information fitting the extreme surges (Villarini et al., 2009).

729 Here, the confidence intervals (CI) have been calculated by the bootstrap technique by  
730 simulating the monthly maxima of surges (spectral component) from the climate index  
731 (spectral component) at each timescale (new samples with a size of 1000). When the original  
732 surges have been fitted to the simulated ones, 95% confidence intervals for the maximum  
733 likelihood estimates have been calculated.

734 (2) a Bayesian estimation has been used to make inferences from the Likelihood function. The  
735 reason behind the choice of this approach is overcoming the limitation of short time-series with  
736 small size, the case of Weymouth station where the measurements covers the period from 1991  
737 and 2018. A technique of Markov Chain Monte Carlo (MCMC), implemented in the evbayes  
738 package within R software, has been used basing on multiple simulations (the number of  
739 simulations is varying as a function of the length of the timeseries).

740 For each spectral component, a sample of 100.000 simulations has been modelled by GEV  
741 using a given climate index. The upper and lower quantiles of the posterior probability  
742 distribution for the parameters of the MCMC sample are taken. The goodness of fit has been  
743 taken as a function of the values of the upper and the lower quantiles; best results have been  
744 considered when these values are higher than 92.5% and lower than 5.2%, respectively.

#### 745 **4. Multi-timescale variability of extreme surges**

746 The variability of the monthly extreme surges along the English Channel coasts has been  
747 investigated using the continuous wavelet transform (CWT). In the spectrum of Figure 2, the  
748 colour scale represents an increasing power (variance) from red to blue and pink. The CWT

749 diagrams highlight the existence of several scales for all sites with different ranges of  
750 frequencies: the interannual scales of ~ 1.5-yr, ~ 2-4-yr, ~ 5-8-yr and the interdecadal scale of  
751 ~ 12-16-yr.

752 The variability of surges is clearly dominated by the interannual frequencies (~ 1.5-yr, ~ 2-4-  
753 yr, ~ 5-8-yr) explaining a mean variance between 32% and 25% of the total energy (Table 1).

754 In Dover and Weymouth, the low frequencies of ~ 2-4-yr are well-structured with a mean  
755 explained variance of 9.5% while it is of 7% for ~ 5-8-yr. These percentages decrease slightly  
756 for the French sites to 8% and 5%, respectively. At ~ 1.5-yr, the explained variance is higher  
757 than 16% and 13% respectively in Britannic and French coasts. The interdecadal frequency of  
758 ~ 12-16-yr varies between 2% and 4% from the total signal. This frequency is not observed in  
759 the shortest timeseries of Weymouth (Table 1).

760 The interannual variability (time-scales higher than ~1 year) seems to be highly represented in  
761 the monthly extrema CWT (Figure 2). It's not the case for the monthly mean surges (Figure  
762 3.a) where most power spectrum is concentrated on the annual cycle with an explained variance  
763 higher than 50%.

764 The time-dependent PDF of the monthly mean and maximum surges over a period of 10 years,  
765 for illustration purpose, is displayed in Figure 3.b. The ~1-yr component of monthly mean

766 surges is largely manifested with a pronounced variation of the Gaussian curves in time; such  
767 variations take wavelengths of approximately  $\sim 2$ -yr and  $\sim 4$ -yr. This result exhibits that the  
768 interannual frequencies of  $\sim 2$ -yr and  $\sim 4$ -yr are modulated within the annual mode for the mean  
769 surges while they are implicitly quantified for the monthly maxima.

770 Results have been explored to investigate the nonstationary dynamics of surges at different  
771 timescales. We have applied the wavelet multiresolution decomposition of monthly extrema  
772 for each site. The process has resulted in the separation of several components with different  
773 time-scales. Only the wavelet components, with have been considered in this work. In this  
774 research, we are interested in the time-scales higher than 1 year, i.e. traduced by three  
775 interannual scales ( $\sim 1.5$ -yr,  $\sim 2$ -4-yr, and  $\sim 5$ -8-yr) and a interdecadal scale of  $\sim 12$ -16-yr. We  
776 focused only on the interannual and the interdecadal scales whose fluctuations correspond to  
777 the oscillation periods less than half the length of the record and exhibit a high-energy  
778 contribution on the variance of the total signal. The lowest frequency, corresponding to  $\sim 12$ -  
779 16-yr is easily calculated from the longest record of Brest.

780 Figure 4 shows a series of oscillatory components of surges from interannual to interdecadal  
781 scales, not easily quantified by a simple visual inspection of the signal. High similarities  
782 between the different sites have been highly observed for the interannual and the interdecadal



783 scales of ~ 5-8-yr and ~12-16-yr while they are less pronounced at the small scales of ~ 1.5-yr.

784 At this timescale, the differences in the extreme surges can be explained by local physical

785 phenomena controlling their dynamics. Such processes are mainly induced by combining the

786 effects of meteorological and oceanographic forces including changes in atmospheric pressures

787 and wind velocities in shallow water areas. Beyond ~ 1.5-yr, the variability of extreme surges

788 at larger scales seems to be quite similar in terms of frequency and amplitude for the five sites.

789 Such large variability reveals the physical effects of a global contribution related to climate

790 oscillations. The extent of the large-scale oscillations is not strictly similar and changes

791 according to the timescale variability since the dynamics of surges is not necessarily related to

792 the same type of atmospheric circulation process. This relationship will be addressed later in

793 the second part of this section.

794 Here, the multiscale variability of extremes has been investigated from the spectral components

795 of surges along the English Channel coasts. This signal has been linearly extracted from the

796 total sea level, provided by tide gauges, by the use of the classical harmonic analysis and thanks

797 to the assumption that the water level is the sum of the mean sea level, tides, and surges. This

798 assumption approximates the quantification of both components in the English Channel where

799 the significant tide-surge interactions (Tomassin & Pirazzoli, 2008) and the effects of the sea-

800 level rise on tides and surges are important (e.g. Idier et al., 2017). Neglecting this nonlinear  
801 interaction between the surges, tides, and the sea-level rise suggests some uncertainties in the  
802 estimation of the high frequencies of the spectral components between daily and monthly  
803 scales, which is not the focus of the present work where the interannual and the interdecadal  
804 scales are investigated.

805 Similar interannual timescales have been observed along the French coasts of Dunkirk, Le  
806 Havre and Cherbourg in Turki et al., (2020) works where the intermonthly and the interannual  
807 variability of 48-year hourly surges has been investigated. They have demonstrated that the  
808 timescales smaller than ~ 1.5-yr are differently manifested between the different sites. These  
809 differences have been associated to the local variability of surges induced by combining the  
810 effects of meteorological and oceanographic forces including changes in atmospheric pressures  
811 and wind velocities in shallow water areas. As demonstrated in Turki et al. (2020) works, the  
812 mean explained variance of the interannual fluctuations (~ 1.5-yr, ~ 2-4-yr, and ~ 5-8-yr) is  
813 around 25% of the total surges along the French coasts (Table 1). This value is higher than 32%  
814 in Weymouth and Dover while the explained variance of the interdecadal scales (~ 12-16-yr)  
815 is also more important with 3.5% (compared to 2% for the French coasts).

816

817 The interdecadal variability (~ 12-16-yr) of extreme surges have been evidenced by Turki et  
818 al., (2019) in the Seine bay (NW France). Strong physical relations have been exhibited  
819 between the interdecadal time of ~ 12-16-yr and the exceptional stormy events produced with  
820 surges higher than 10-year return period level. The connections between the low-frequency  
821 components and the historical record of the exceptional events suggested that storms would  
822 occur differently according to a series of physical processes oscillating at multi-timescales;  
823 these processes control their frequency and their intensity (Turki et al., 2019).

824 .

825 Accordingly, the multiscale variability of extreme surges exhibits a nonstationary behaviour  
826 modulated by a non-linear interaction between the different interannual and the interdecadal  
827 timescales. Then, assessing the effect of the nonstationary behaviour at different timescales is  
828 important for improving the estimation of extreme values and the projection of storm surges.

829

## 830 **5. Large-scale climate North-Atlantic oscillations and their link to** 831 **extreme surges in the English Channel**

832

833 In this part, a new hybrid approach combining the spectral analysis and the nonstationary GEV  
834 models has been used to investigate the connection between the multi-timescale variability of  
835 local surges and the large-scale climate North Atlantic oscillations.

836 As proposed by Turki et al. (2019; 2020), the hypothesis used in the present work is that the  
837 multi-timescale variability of the local extreme surges should be strongly related to different  
838 climate teleconnections induced by a complex contribution of many physical mechanisms. This  
839 non-linear relationship varies according to each timescale which depends on a specific large-  
840 scale oscillation of atmospheric circulation.

841

### 842 ***5.1 To what extent would large-scale climate oscillations link extreme surges?***

843 The wavelet coherence (WC) diagrams between the monthly maxima of surges and the  
844 different climate indices of SLP, ZW, NAO, AMO, introduced previously as the main  
845 atmospheric circulation within the English Channel, are illustrated respectively in Figures 5, 6,  
846 7 and 8. Results provided by these diagrams highlight:

- 847 1. The connection between the climate oscillations and the extreme surges is manifested  
848 differently as a function of the timescale. From a visual inspection of the different  
849 spectra provided WC, the most significant correlations of extreme surges have been

850 identified with SLP, ZW, NAO and AMO respectively at ~ 1.5-yr, ~ 2-4-yr, ~ 5-8-yr  
851 and ~ 12-16-yr.

852 2. Each timescale exhibits mainly strong links with its associated climate index (explained  
853 variance varying between 55% and 80%) and weak ones with other indices (explained  
854 variance varying between 15% and 5%). Table 2 summarizes the contribution of the  
855 different climate oscillations in the different interannual and interdecadal timescales of  
856 extreme surges. Here, mean values between the different sites are presented.

857 For example, SLP diagrams reveal significant relationships with ~ 1.5-yr surges (well-  
858 structured forms with high concentration of pink-blue colours in Figure 5); limited  
859 correlations, locally positioned in time, have been observed at ~ 2-4-yr and ~ 5-8-yr scales.  
860 ZW shows strong correlations with interannual surges at ~ 2-4-yr (blue to pink colour at  
861 this scale; Figure 6) and others correlations at smaller and larger timescales of ~ 1.5-yr and  
862 ~ 5-8-yr, respectively. Similarly, NAO presents high links with ~ 5-8-yr surges and small  
863 relations with ~ 2-4-yr and ~ 1.5-yr (Figure 7).

864 The ~ 1.5-yr scale highlights strong correlations with SLP with an explained variance of 75%;  
865 25% of this scale should be explained by the influence of other climate oscillations (basically

866 ZW and NAO with a mean explained variance of 10% and 6%, respectively; Table 2) and the  
867 combining effects of local driven forcing induced by winds and waves.

868 65% of ~ 2-4-yr scale is correlated with ZW while 5% and 12% is explained by the effect of  
869 NAO and SLP, respectively. The effects of NAO on the ~ 5-8-yr vary between 55% and 65%;  
870 minor influence at this scale has been observed with SLP and ZW explaining a mean variance  
871 of 13%. The interannual scales of surges are slightly influenced by AMO oscillations with low  
872 values of variance lower than 1% (Table 2).

873 At interdecadal scales of ~ 12-16-yr, the extreme surges are mainly controlled by the AMO  
874 oscillations with a mean explained variance of 80% while the effects of NAO is limited to 10%.

875 Figure 9 displays the spectral components of the four climate oscillations, provided by a multi-  
876 resolution analysis, together with the spectral components extracted from the extreme surges  
877 (Figure 4) with the aim to quantify the different connections between both variables at the  
878 interannual and the interdecadal timescales.

879 [For each timescale, a bootstrap approach has been applied to assess the statistical significance](#)  
880 [of the correlation between the spectral component of the extreme surges and the climate](#)  
881 [oscillation. By resampling the timeseries 10.000 times, 95% confidence intervals have been](#)  
882 [considered to extract the best climate information fitting the extreme surges \(Villarini et al.,](#)  
883 [2009\).](#)

884

885 The best correlation of each surge component (i.e. ~ 1.5-yr, ~ 2-4-yr, ~ 5-8-yr and ~ 12-16-yr)  
886 with the suitable climate index ( i.e. SLP, ZW, NAO and AMO) is illustrated in Figure 9.

887 The interannual and the interdecadal variability of extreme surges and their multiscale  
888 connection with the climate oscillations highlight the nonlinear relationship between large- and  
889 local- scales.

890 Therefore, the interannual and the interdecadal extreme surges have proven to be strongly  
891 related to different composites of oscillating atmospheric patterns. Such composites seem to be  
892 not necessarily similar for the different timescales. The use of a multiresolution approach to  
893 investigate the dynamics of the extreme surges into the downscaling studies proves to be useful  
894 for assessing the nonstationary dynamics of the local extreme surges and their nonlinear  
895 interactions with the large-scale physical mechanisms related to climate oscillations.

896 Investigating the complex relationships between the climate oscillations and the multi-  
897 timescale surges has exhibited a multimodel climate ensemble that should be used to better  
898 understand this complexity.

899 The interannual connections between the local hydrodynamics and the climate variability have  
900 been investigated in numerous previous works focused on the atmospheric circulation with

901 different related mechanisms (e.g., Feliks et al., 2011; Lopez-Parages et al. 2012; Zampieri et  
902 al., 2017). As demonstrated by the recent works of Turki et al. (2019, 2020), the effects of SLP  
903 oscillations on the  $\sim 1.5$ -yr variability of extreme surges are described by dipolar patterns of  
904 high-low pressures with a series of anomalies which are probably induced by some physical  
905 mechanisms linked to the North-Atlantic and ocean/atmospheric circulation oscillating at the  
906 same timescale.

907 The SLP fields combined with the baroclinic instability of wind stress have been related to the  
908 Gulf Stream path as given by NCEP reanalysis (Frankignoul et al., 2011); the dominant signal  
909 is a northward (southward) displacement of the Gulf Stream when the NAO reaches positive  
910 (negative) extrema. Daily mean SLP fields have been used by Zampieri et al. (2017) to analyse  
911 the influence of the Atlantic sea temperature variability on the day-by-day sequence of large-  
912 scale atmospheric circulation patterns over the Euro-Atlantic region. They have associated the  
913 significant changes in certain weather regime frequencies to the phase shifts of the AMO. For  
914 hydrological applications, several works have investigated the multiscale relationships between  
915 the local hydrological changes and the climate variability. Lavers et al. (2010) associated the  
916 7.2-yr timescales to SLP patterns which are not exactly reminiscent of the NAO and define  
917 centers of action which are shifted to the North.



918 Regarding the ZW (u850), results have shown its correlation with the interannual scales of ~2-  
919 4-yr extreme surges as suggested also in the recent findings of Turki et al. (2020). Its influence  
920 has been proven also at smaller (~1.5-yr) and larger scales (5-8-yr). Additionally, to extreme  
921 surges, the interaction between the ZW and the temperature at different timescales has been  
922 highlighted in some previous researches (e.g., Andrade et al., 2012; Seager et al. 2003;  
923 Woodworth et al., 2007). Along UK and Northern English Channel coasts, Changes in trends  
924 of extreme waters and storm surges have been explained by variations of energy pressure and  
925 ZW variability additional to thermosteric fluctuations linked to NAO (Woodworth et al., 2007).  
926 Andrade et al. (2012) have used the component of ZW at 850 hPa to investigate the positive  
927 and the negative phases of the extreme temperatures in Europe and their occurrence in relation  
928 with the large-scale atmospheric circulation. They suggested that both phases are commonly  
929 connected to strong large-scale changes in zonal and meridional transports of heat and  
930 moisture, resulting in changes in the temperature patterns over western and central Europe  
931 (Corte-Real et al., 1995; Trigo et al., 2002). The physical connections between ZW and the  
932 extreme events from 11 Global Climate Model runs have been demonstrated by the studies  
933 from Mizuta (2012) and Zappa et al (2013); they have suggested the complex relationship  
934 between the climate oscillation and the jet stream activity. They have found a slight increase

935 in the frequency and strength of the storms over the central Europe and decreases in the number  
936 of the storms over the Norwegian and Mediterranean seas.

937 The NAO is considered as an influencing climate driver for the large-scale atmospheric  
938 circulation, as suggested by other researches (e.g. Marcos et al., 2009; Philips et al., 2013).

939 The existence of long-term oscillations originating from large-scale climate variability and thus  
940 controlling the interannual extreme surges has been highlighted from investigating the low  
941 frequencies of the sea levels along the English Channel. This is in agreements with the results  
942 recently demonstrated by Turki et al. (2020) and the present finding exhibiting the strong links  
943 between NAO oscillations and the ~ 5-8-yr extreme surges along the English Channel coasts.

944 The physical mechanisms related to the effects of the continuous changes in NAO patterns on  
945 the sea-level variability have been addressed in several studies (e.g., Marcos et al., 2005;  
946 Tsimplis et al., 1994). At the interannual scales, the key role of NAO on the sea-level variability  
947 has been explained by some previous works: Philips et al. (2013) investigated the influence of  
948 the NAO on the mean and the maximum extreme sea levels in the Bristol Channel/Severn  
949 Estuary. They have demonstrated that when high NAO winters increase in the positive phase,  
950 wind speeds also escalate while increasing the negative NAO winters results in low wind  
951 speeds. Then, the correlation between the low/high extreme surges and the NAO in the Atlantic

952 has demonstrated a proportionality between NAO values and the augmentation in the winter  
953 storms. Feliks et al. (2011) defined significant oscillatory timescales of ~ 2.8-yr, ~ 4.2-yr, and  
954 ~ 5.8-yr from both observed NAO index and NAO atmospheric marine boundary layer  
955 simulations forced with SST; they have suggested that the atmospheric oscillatory modes  
956 should be induced by the Gulf Stream oceanic front.

957 Strong correlations between the monthly extreme surges and the AMO oscillations have been  
958 identified at the timescale of 12-16-yr (Figure 8 and Figure 9; in particular for Brest). Since the  
959 period of 1990's, the AMO and the extreme surges oscillate in opposition of phase. This shift  
960 should be explained by a substantial change in European climate manifested by cold wet and  
961 hot dry summers in the northern and the southern Europe, respectively; as discussed by Sutton  
962 and Dong (2012). They have demonstrated that the patterns, identified from the European  
963 climate change around 1990's, are synchronised with changes related to the North Atlantic  
964 Ocean.

965 Other weak links with the AMO have been identified at the interannual timescales of ~5-8-yr.  
966 along the studied sites. In agreement of previous works (e.g., Enfield et al., 2001; Zampieri et  
967 al., 2013; 2017), the effects of the AMO oscillations are mainly manifested at the interannual  
968 timescales to control the variability of hydrological (e.g. rainfall) and oceanographic (e.g.  
969 surges) variables. Generally, the climate oscillations of AMO are associated to the SST  
970 variability with a time cyclicity of about 65-70-years (e.g. Delworth and Mann, 2000; Enfield  
971 et al., 2001). During the warming periods of the 1990's, the AMO shifts from the negative to  
972 the positive phases in the Northern Hemisphere corresponding to cold and warm periods (e.g.

973 Gastineau et al., 2012; Zhang et al., 2013). This shift can be responsible on changes in the  
974 hydrodynamic conditions (e.g. Zampieri et al., 2013).

975 The influence of the AMO oceanic low frequencies in the modulation of the mechanisms of  
976 the atmospheric teleconnections at the interannual timescales has been investigated in many  
977 previous works (e.g Enfield et al. 2001). At decadal timescales, the existing relationships  
978 between the winter NAO and the AMO variability is more complex (e.g. Peings and  
979 Magnusdottir, 2014).

980 The effects of the AMO-driven climate variability on the seasonal weather patterns have been  
981 investigated by Zampieri et al. (2017) in Europe and the Mediterranean. They have  
982 demonstrated significant changes in the frequencies of weather regimes involved by the AMO  
983 shifts which are in phase with seasonal surface pressure and temperature anomalies. Such  
984 regimes, produced in Spring and Summer periods, are differently manifested in Europe with  
985 anomalous cold conditions over Western Europe (Cassou et al., 2005; Zampieri et al., 2017).

986 In summary, four atmospheric oscillations have proven to be significantly linked to the  
987 interannual and interdecadal variability of extreme surges. This physical link varies according  
988 to the timescale exhibiting a nonlinear interaction of the same oscillations with other scales.

989 Such nonlinear behavior depends on the dynamics of the different sequences of the atmospheric  
990 and water vapour transport patterns during the month prior to the sea-level observations (e.g.

991 Lavers et al., 2015). As suggested by Turki et al. (2020), the atmospheric circulation acts as a  
992 regulator controlling the multiscale variability of extreme surges with a nonlinear connection

993 between the large-scale atmospheric circulation and the local scale hydrodynamics. This multi-

994 timescale dependence between the local extreme dynamics and the internal modes of climate  
995 oscillations is still under debate. Understanding these physical links, even their complexities,  
996 are useful to improve the estimation of the extreme values in coastal environments; which is  
997 the objective of the next part.

## 998 ***5.2 Nonstationary modelling of extreme surges***

999 In this part, stationary and nonstationary extreme value analyses based on GEV distribution  
1000 with time-dependent parameters (Coles, 2001) have been implemented to model separately the  
1001 different spectral components of extreme surges. Four GEV stationary (GEV0) and  
1002 nonstationary (GEV1, GEV2 and GEV3) models have been applied to each timescale and each  
1003 site. The GEV distribution uses the maximum likelihood method by parametrizing the location,  
1004 scale, and shape of the model. We have used the ‘trust region reflective algorithm’ for  
1005 maximizing the log-likelihood function (Coleman and Li, 1996).

1006 The connections between the climate oscillations and the monthly maxima at the different  
1007 timescales (Figure 9), presented previously (section 5.1), have been explored as a first  
1008 hypothesis for the implementation of the nonstationary GEV models. Indeed, multiple  
1009 simulations of Markov Chain Monte Carlo (MCMC) techniques based on Bayesian approaches  
1010 have been employed for extreme surge components (i.e. ~ 1.5-yr, ~ 2-4-yr, ~ 5-8-yr and ~ 12-

1011 16-yr provided by the multiresolution wavelet decomposition) to identify the best covariates of  
1012 climate oscillation for parametrizing the nonstationary GEV models. The most of simulations  
1013 has mainly supported the results outlined in the previous section: the ~ 1.5-yr of SLP, ~ 2-4-  
1014 yr of ZW, ~ 5-8-yr of NAO and ~ 12-16-yr of AMO oscillations are considered as the best  
1015 covariates for modelling respectively the ~ 1.5-yr, ~ 2-4-yr, ~ 5-8-yr and ~ 12-16-yr of monthly  
1016 extreme surges.

1017 Once the climate covariate has been selected for each timescale, three nonstationary models  
1018 have been used by introducing the climate information as a covariate into: (1) the location  
1019 parameter (GEV1); (2) both location and scale parameters (GEV2); (3) all location, scale and  
1020 shape parameters (GEV3). The structure of the most appropriate nonstationary GEV  
1021 distribution has been selected by choosing the most adequate parametrization that minimizes  
1022 the Akaike information criterion (Akaike, 1974). The goodness of fit for each model has been  
1023 checked through the visual inspection of the quantile-quantile (Q-Q) plots (Figure 10); these  
1024 plots compare the empirical quantiles against the quantiles of the fitted model. Any substantial  
1025 departure from the diagonal indicates inadequacy of the GEV model.

1026

1027 At the interannual scales and for all sites, results provided by the nonstationary GEV1-3 reveal  
1028 a better performance (the lowest values of AIC) of extreme estimation compared to the  
1029 stationary models of GEV0 and give the most appropriate distributions by the use of the climate  
1030 large-scale covariates for specific oscillating components of extreme surges. Nevertheless, this  
1031 improvement from the stationary to the nonstationary models has not been clearly observed for  
1032 the interdecadal scales where the extreme estimation, provided by the different GEV models,  
1033 is very similar (Table 3). The lowest values of AIC have been shown by GEV3 for ~1.5-yr,  
1034 GEV2 for ~2-4-yr and GEV1 for ~5-8-yr (Table 4). The Q-Q plots for the all timescales of all  
1035 timescales of the monthly maxima in Brest are illustrated in Figure 10; they confirm the  
1036 suitability of the selected models.

1037 Accordingly, the nonstationary GEV models have exhibited high improvements at the  
1038 interannual scales where the AIC scores have significantly decreased by introducing the  
1039 climate information into the parametrization of the model. Such consideration varies as a  
1040 function of the spectral components, it concerns all parameters for the smallest scale of ~1.5-  
1041 yr, both location and scale parameters for ~2-4-yr and only the location parameter for largest  
1042 scale of ~5-8-yr.

1043 Then, the large-scale oscillations introduced for the implementation of GEV parameters depend  
1044 on the time scale for all sites exhibiting a high nonstationary behaviour of the small interannual  
1045 scales (~1.5-yr) which decreases at the large interannual scales (~5-8-yr) and get non-  
1046 significant at the interdecadal scales (~ 12-16-yr).

1047 The use of the time-varying GEV parameters at the interannual scales (~ 1.5-yr and ~ 2-4-yr)  
1048 exhibits the relationship between the mode and the standard deviation of the GEV distributions  
1049 associated with the location and the scale parameters, respectively.

1050 The different implications of both parameters for estimating the interannual extreme surges  
1051 reveal cyclic variations and timescale modulations related to the large-scale climate  
1052 oscillations. As documented in the previous works (e.g., Menendez et al., 2009; Masina and  
1053 Lamberti., 2013), the location and the scale parameters used for improving the nonstationary  
1054 estimation of the extreme water levels highlight a series of annual and semi-annual evolutions.

1055 They have reported that the seasonal cycles of the location parameter are related to tow maxima  
1056 of water levels, in early March and September produced during equinoctial spring tides, while  
1057 the seasonal cycles of the scale parameter are associated to an increase of storms during wintry  
1058 episodes. Here, we focus on the stochastic signal of surges at scales larger than one year. The  
1059 SLP and the ZW frequencies, introduced in the location and the scale parameters of



1060 nonstationary GEV models, determine an enhancement in the prediction of the interannual  
1061 scales.

1062 The shape parameter, implied for the estimation of the ~1.5-yr extreme surges, derives from its  
1063 determination of the upper tail distribution behaviour. The time-varying shape parameter uses  
1064 the ~1.5-yr SLP exhibiting altering negative and positive oscillations.

1065 Despite its critical significance, the shape GEV parameter has revealed its relationships with  
1066 basin attributes in hydrological applications and regional flood frequency analysis (e.g., Tyrallis  
1067 et al., 2019). The dependence of the shape parameter on the climate oscillations has been  
1068 demonstrated in several extreme frameworks related to hydrological and oceanographic  
1069 applications (e.g., Menendez et al., 2009; Masina et al., 2013; Turki et al., 2020). Regarding  
1070 the stationarity of the surge timescale, the ~12-16-yr window sliding matches have been  
1071 quantified in the previous part exhibiting a substantial cyclic variability consequence of an  
1072 altering periods of positive and negative correlations. The modelling of the interdecadal  
1073 extreme surges involves a stationary behavior of the ~12-16-yr.

1074 Th stationary behavior of low frequencies has been outlined by Zampieri et al. (2017). They  
1075 have demonstrated a stationary trend of the SST anomalies associated with the AMO over the  
1076 Euro-Atlantic region. According to their works, the low-frequency variability of the European  
1077 Climate is influenced by the AMO shift induced by the phase opposition between the negative  
1078 NAO distribution and the Atlantic patterns.

1079 [Here, the effects of AMO on ~12-16-yr of extreme surges have been largely observed in Figure](#)  
1080 [9 for the longer timeseries Brest where the lower frequencies could be easily identified.](#)

1081

1082 [At this timescale, the AIC values given by the different GEV models are pretty close and the](#)  
1083 [difference between the distributions are not statistically significant. The stationary behavior of](#)  
1084 [~12-16-yr surges should be more investigated from additional applications in light of the](#)  
1085 [available sea level measurements covering a long period of time, a relevant parameter to](#)  
1086 [characterize the uncertainties in extreme value statistical modeling of flood hazards.](#)

1087

1088 The return levels of the multiscale extreme surges, provided by the best GEV models (Table  
1089 3), have been simulated. The example of Brest is illustrated in Figure 10.b for the interannual  
1090 (nonstationary GEV models) and the interdecadal (GEV stationary model) scales. The 95%  
1091 confidence interval is also plotted in this graph through a dashed black line. Accordingly, the  
1092 use of GEV distribution with time-dependent parameters for each timescale should improve  
1093 the evaluation of the return values and reduce the uncertainty of the quantile estimates.

1094 [Similar works have been carried out by Wahls and Chambers \(2016\) to investigate the](#)  
1095 [multidecadal variations in extreme sea levels with the large-scale climate variability. By the](#)  
1096 [use of climate indices on nearby atmospheric/oceanic variables \(winds, pressure, sea surface](#)  
1097 [temperature\) as covariates in a quasi-nonstationary extreme value analysis, the range of change](#)  
1098 [in the 100-year return water levels has been significantly reduced over time, turning a](#)  
1099 [nonstationary process into a stationary one.](#)

1100

1101 [As suggested by Wong \(2018\), including a wider range of physical process information and](#)  
1102 [considering nonstationary behaviour can better enable modelling efforts to inform coastal risk](#)  
1103 [management. In his work, he has developed a new approach to integrate stationary and](#)  
1104 [nonstationary statistical models and demonstrated that the choice of covariate timeseries should](#)  
1105 [affect the projected flood hazards. By developing a nonstationary storm surge statistical model](#)  
1106 [with the use of multiple covariate timeseries \(global mean temperature, sea level, the North](#)

1107 Atlantic Oscillation index and time) in Norfolk and Virginia, he has shown that a storm surge  
1108 model raises the projected 100-year storm surge return level by up to 23 cm relative to a  
1109 stationary model or one that employs a single covariate timeseries.

1110 This study has expanded the previous works of Turki et al. (2019; 2020) upon a new approach  
1111 combining spectral and probabilistic methods to integrate multiple streams of information  
1112 related to climate teleconnections. Indeed, each timescale has been simulated separately with  
1113 the nonstationary GEV models and expressed as a function of the most suitable climate index  
1114 improving its fitting. The estimation of the total signal of surges should be determined by  
1115 combining the developed nonstationary GEV models used for the different timescales.

1116 These results should support the hypothesis introduced at the beginning of the present work  
1117 suggesting that: (i) the extreme surges should depend on different timescales; (ii) each  
1118 timescale should be related to a specific large-scale oscillation.

1119 The finding is in agreement with the previous works of Lee et al. (2017) and Wang et al. (2018)  
1120 highlighting the importance of a careful consideration when complex physical mechanisms of  
1121 different climate indices are included into model structures for estimating extreme surges.  
1122 Indeed, this work provides a guidance on incorporating nonstationary processes of large-scale  
1123 oscillations to different spectral components informed by the wavelet techniques, the Bayesian  
1124 approaches and the GEV model probabilities.

1125 The primary contribution of the present research is to present a new approach for: (1)  
1126 investigating the multi-timescale variability of the nonstationary extreme surges; (2)  
1127 identifying their multi-connection with climate oscillations according to the timescale and (3)  
1128 resolve in part the problems of uncertainty of most appropriate climate to use as covariate for  
1129 GEV models at each timescale. However, additional models (e.g. significance tests and  
1130 sensitivity analyses and modelling uncertainties) and application sites (e.g. Mediterranean and

1131 [pacific ones controlled by other climate oscillations\) are required to expand the developed](#)  
1132 [approach.](#)  
1133 [Also, generating a final robust stochastic model useful for projecting storm surge return levels](#)  
1134 [and assessing the flood risk management requires further efforts to build on the potentially](#)  
1135 [advantageous approach presented here by integrating the GEV models associated with the](#)  
1136 [different timescales through the use of mathematical methods.](#)

1137  
1138  
1139

## 6. Summary and Concluding remarks

1140 The dynamics of extreme surges together with the large-scale climate oscillations have been  
1141 investigated by the use of hybrid methodological approach combining spectral analyses and  
1142 nonstationary GEV models. Results have demonstrated that the interannual variability of  
1143 extreme surges (~ 1.5-yr, ~2-4-yr and 5-8-yr) is around 25% for the French coasts and higher  
1144 than 32% for the Britannic coasts; the interdecadal variability (~12-16-yr) varies between 2%  
1145 and 4%. The fluctuations of extreme surges at ~1.5-yr are differently manifested between the  
1146 different sites of the English Channel exhibiting a local variability of surges induced by the  
1147 effects of meteorological and oceanographic forces including changes in atmospheric pressures  
1148 and wind velocities in shallow water areas. Similar fluctuations have been observed at larger  
1149 scales of the interannual and the interdecadal variability. Changes in extreme surges (~1.5-yr,  
1150 ~2-4-yr, ~5-8-yr and ~12-16-yr) have been proven to be significantly linked to atmospheric

1151 oscillations (SLP, ZW, NAO and AMO, respectively) according to the timescale with a  
1152 nonlinear interaction between different oscillations at the same scale. This exhibits the complex  
1153 physical mechanisms of the global atmospheric circulation acting as a regulator and controlling  
1154 the local variability of extreme surges at different timescales. The connections between the  
1155 multiscale extreme surges and the internal modes of climate oscillations have been explored to  
1156 improve the estimation of extreme values by the use of nonstationary GEV models. The  
1157 simulated extreme surges have highlighted that introducing the climate oscillations for the  
1158 implementation of GEV parameters depends on the timescale for all sites; a high nonstationary  
1159 behaviour of the small interannual scales (~1.5-yr) decreases at the larger scales (~5-8-yr) and  
1160 seems to be non-significant at the interdecadal scales (~ 12-16-yr).

1161 The conclusion of this research suggests that the physical mechanisms driven by the  
1162 atmospheric circulation, including the Gulf Stream gradients, play a key role in coastal extreme  
1163 surges. Establishing a strong connection of the large-scale climate oscillations with extreme  
1164 surges and flooding risks improve the estimation of the return levels.

1165 This finding presents a handful of a new approach potentially useful as a first step forward for  
1166 (1) understanding the physical relation of downscaling from the global climate patterns to the  
1167 local extreme surges; (2) inferring the future projections of sea level change and extreme

1168 events. Future work should build on this new approach to (1) improve the stochastic modelling  
1169 of the multi-timescale extreme surges; (2) incorporate others climate mechanisms known to be  
1170 important at local and regional scales for specific applications; (3) generate a robust tool for  
1171 the storm surge projections and the flood risk assessments based on the different timescale  
1172 models connected to their specific climate drivers.

### 1173 **Acknowledgments**

1174 The research programs ‘RICOCHET’, ‘RAIV COT’, ‘REVE COT’ and CNES-TOSCA  
1175 ‘COTEST’ are acknowledged for funding this research. elated to the future mission of Surface  
1176 Water and Ocean Topography (SWOT). We also acknowledge the National Navy  
1177 Hydrographic Service (SHOM), the British Oceanographic Data Center and the National  
1178 Center for Environmental Prediction for providing sea level and atmospheric data.

### 1179 **References**

1180 Akaike, H.: Information theory as an extension of the maximum likelihood principle. In:  
1181 Petrov, B. N., and Csaki, F. (Eds.), Second International Symposium on Information Theory,  
1182 Akademiai Kiado, Budapest, pp. 267–281, 1974.  
1183 Andrade, C., Leite, S. M., and Santos, J. A.: Temperature extremes in Europe: overview of  
1184 their driving atmospheric patterns. *Natural Hazards Earth System Sciences*, 12, 1671–1691,  
1185 <https://doi.org/10.5194/nhess-12-1671-2012>, 2012.

1186 Bell, R., G., and Goring, D., G.: Seasonal Variability of Sea Level and Sea-surface Temperature  
1187 on the North-east Coast of New Zealand. *Estuarine, Coastal and Shelf Science*, 46 (2), 307-  
1188 319, <https://doi.org/10.1006/ecss.1997.0286>, 1998.

1189 Bessoumoulin, P.: Les tempêtes en France. *Annales des Mines*. 9-14, 2002.

1190 Brown, J., Souza, A., and Wolf, J.: Surge modelling in the eastern Irish Sea: Present and future  
1191 storm impact, *Ocean Dynamics* 60(2), 227–236, doi:10.1007/s10236-009-0248-8, 2010.

1192 Carter, D. J. T., and Challenor, P.G.: Estimating return values of environmental parameters.  
1193 *Quarterly Journal of the Royal Meteorological Society*, 107, 259-266, 1981.

1194 Caspar, R., Costa, S., Lebreton, P., and Letortu, P.: Storm surges of the 10-11 march 2008 on  
1195 the Albâtre Coast (Haute-Normandy, France): meteo-marine determination. *NOROIS*, p.115-  
1196 132, <https://doi.org/10.4000/norois.3273>, 2010

1197

1198 Cassou, C., Terray, L., and Phillips, A.S.: Tropical Atlantic influence on European heat waves.  
1199 *Journal of Climate*, 18, 2805–2810, 2005.

1200 Ciasto, L.M., and Thompson, D.W.J.: North Atlantic Atmosphere-Ocean Interaction on  
1201 Intraseasonal Time Scales. *Journal of Climate*, 17, 1617 – 1621, 2004.

1202 ey, D. et al.: “Bayesian spatial modelling of extreme precipitation return levels” . *Journal of*  
1203 *American Statistical Association*, 102: 824-840, 2007.

1204 Colberg, F., McInnes, K.L., Grady, J., and Hoeke, R.: Atmospheric circulation changes and  
1205 their impact on extreme sea levels around Australia. *Natural Hazards Earth System Sciences*,  
1206 19, 1067–1086. <https://doi.org/10.5194/nhess-19-1067-2019>, 2019.

1207 Coleman, T. F., Li, Y.: An interior trust region approach for nonlinear minimization subject  
1208 to bounds. *SIAM Journal on Optimization*, 6(2), 418-445. doi:10.1137/0806023, 1996.

1209 Coles, S.: *An Introduction to Statistical Modelling of Extreme Values*, Springer, London, U.  
1210 K., 2001.

1211 Collier, J.S., Oggioni, F., Gupta, S., García-Moreno, D., Trentesaux, A., and De Batist, M.:  
1212 Streamlined Islands and the English Channel Megaflood Hypothesis. *Global and Planetary*  
1213 *Change*, 135, 190–206. <https://doi.org/10.1016/j.gloplacha.2015.11.004>, 2015.

1214 Corte-Real, J., Zhang, Z., and Wang, X.: Large-scale circulation regimes and surface climatic  
1215 anomalies over the Mediterranean. *International Journal of Climatology*, 15, 1135–1150,  
1216 <https://doi.org/10.1002/joc.3370151006>, 1995.

1217 Enfield, D.B., Mesta-Nunez, A.M., and Trimble, P.J.: The Atlantic multidecadal oscillation  
1218 and its relation to rainfall and river flows in the continental U.S. *Geophysical Research Letters*,  
1219 28 (10), 2077–2080, 2001.

1220 Delworth, T.L., and Mann, M.E.: Observed and simulated multidecadal variability in the  
1221 Northern Atlantic. *Climate Dynamics*. 16, 661–676, 2002.

1222 Feliks, Y., Ghil, M., and Robertson, A.W.: The atmospheric circulation over the North Atlantic  
1223 as induced by the SST field. *Journal of Climate*, 4 (2), 522–542,  
1224 <http://dx.doi.org/10.1175/2010JCLI3859.1>, 2001.

1225 Frankignoul, C., N. Sennechael, Y., Kwon, O., and Alexander, M.A.: Influence of the  
1226 Meridional Shifts of the Kuroshio and the Oyashio Extensions on the Atmospheric Circulation.  
1227 *Journal of Climate*, 24, 762 – 777, <https://doi.org/10.1175/2010JCLI3731.1>, 2011.

1228 Gastineau, G., D'Andrea, F., and Frankignoul, C.: Atmospheric response to the North Atlantic  
1229 Ocean variability on seasonal to decadal time scales. *Climate Dynamics*, 2012.

1230 Grinsted A, Moore J, Jevrejeva S: Application of the crosswavelet transform and wavelet  
1231 coherence to geophysical time series. *Nonlinear Processes in Geophysics* 11(5): 561–566,  
1232 2004.

1233 Gupta, S., Collier, J.S., Andy, P.F., and Potter, G.: Catastrophic Flooding Origin of Shelf  
1234 Valley Systems in the English Channel. *Nature*, 448 (7151): 342–45.  
1235 <https://doi.org/10.1038/nature06018>, 2007.



1236 Haigh, I., Nicolls, R., and Wells, N.: Assessing changes in extreme sea levels: Application to  
1237 the English Channel 1900-2006. *Continental Shelf Research*, 30, 1042-1055.  
1238 <https://doi.org/10.1016/j.csr.2010.02.002>, 2010.

1239 Haigh, I., Nicolls, R., and Wells, N.: Mean sea level trends around the English Channel over  
1240 the 20<sup>th</sup> century and their wider context. *Continental Shelf Research*, 29, 2083-2098.  
1241 <https://doi.org/10.1016/j.csr.2009.07.013>, 2009.

1242 Hanson, S., Nicholls, R., Ranger, N., Hallegatte, S., Dorfee-Morlot, J., Herweijer, C., and  
1243 Chateau, J.: A global ranking of port cities with high exposure to climate extremes. *Climate*  
1244 *Change*, 104(1), 89-111, [10.1007/s10584-010-9977-4](https://doi.org/10.1007/s10584-010-9977-4), 2011.

1245 Idier, D., Dumas, F., and Muller, H.: Tide-surge interaction in the English Channel. *Natural*  
1246 *Hazards Earth System Sciences*, 12, 3709–3718. doi:10.5194/nhess-12-3709-2012, 2012.

1247 Idier, D., Paris, F., Le Cozannet, G., Boulahya, F., and Dumas, F.: Sea-level rise impacts on  
1248 the tides of the European Shelf, *Continental Shelf Research*, 56-71.  
1249 <https://doi.org/10.1016/j.csr.2017.01.007>, 2017.

1250

1251 Labat, D.: Recent advances in wavelet analyses: Part 1. A review of concepts. *Journal of*  
1252 *Hydrology*, 314 (1–4), 275–288. <http://dx.doi.org/10.1016/j.jhydrol.2005.04.003>, 2005.

1253 Lavers, D.A., Hannah, D.M., and Bradley, C.: Connecting large-scale atmospheric circulation,  
1254 river flow and groundwater levels in a chalk catchment in southern England. *Journal of*  
1255 *Hydrology*, 523, 179–189. <http://dx.doi.org/10.1016/j.jhydrol.2015.01.060>, 2015.

1256

1257 Lavers, D.A., Prudhomme, C., and Hannah, D.M.: Large-scale climate, precipitation and  
1258 British river flows: Identifying hydroclimatological connections and dynamics. *Journal of*  
1259 *Hydrology*, 395 (3–4), 242–255. <https://doi.org/10.1016/j.jhydrol.2010.10.036>, 2010.

1260

1261 Lee, B. S., Haran, M., and Keller, K.: Multi-decadal scale detection time for potentially  
1262 increasing Atlantic storm surges in a warming climate, *Geophysical Research Letters.*, 44,  
1263 10617–10623, <https://doi.org/10.1002/2017GL074606>, 2017.

1264

1265 López-Parages, J., and Rodríguez-Fonseca, B.: Multidecadal modulation of El Niño influence  
1266 on the Euro-Mediterranean rainfall. *Geophysical Research Letters*, 39:L02704,  
1267 <https://doi.org/10.1029/2011GL050049>, 2012.

1268 Marcos, M., Calafat, F. M., Berihuete, A., and Dangendorf, S: Long-term variations in global  
1269 sea level extremes. *Journal of Geophysical Research, Oceans*, 120, 8115- 8134,  
1270 [doi:10.1002/2015JC011173](https://doi.org/10.1002/2015JC011173), 2015.

1271

1272 Marcos, M., and Woodworth, P. L: Spatiotemporal changes in extreme sea levels along the  
1273 coasts of the North Atlantic and the Gulf of Mexico. *Journal of Geophysical Research, Oceans*,  
1274 122, 7031-7048, [doi:10.1002/2017JC013065](https://doi.org/10.1002/2017JC013065), 2017.

1275 Masina M., and Lamberti A.: A nonstationary analysis for the Northern Adriatic extreme sea  
1276 levels, *Journal of Geophysical Research*, 118, <https://doi.org/10.1002/jgrc.20313>, 2013.

1277 Massei, N., Durand, A., Deloffre, J., Dupont, J., Valdes, D., and Laignel, B.: Investigating  
1278 possible links between the North Atlantic Oscillation and rainfall variability in northwestern  
1279 France over the past 35 years. *Journal of Geophysical Research - Atmosphere*, 112, 1–10,  
1280 <https://doi.org/10.1029/2005JD007000>, 2007.

1281 Massei, N., Laignel, B., Deloffre, J., Mesquita, J., Moyelay, A., and Lafite, R., Durant, A.:  
1282 Long-term hydrological changes of the Seine River flow [France] and their relation to the North  
1283 Atlantic Oscillation over the period 1950-2008. *International Journal of Climatology*, 29,  
1284 <https://doi.org/10.1002/joc.2022>, 2009.

1285 Massei, N., Dieppois, B., Hannah. D. M., Lavers, D.A., Fossa, M., Laignel, B., and Debret, M.:  
1286 Multi-time-scale hydroclimate dynamics of a regional watershed and links to large-scale  
1287 atmospheric circulation: Application to the Seine river catchment, France. *Journal of*  
1288 *Hydrology*, 546; 262-275, <https://doi.org/10.1016/j.jhydrol.2012.04.052>, 2017.

1289 Menendez M., and Woodworth P. L.: Changes in extreme high-water levels based on a quasi-  
1290 global tide-gauge data set, *Journal of Geophysical Research*, 115, C10011.  
1291 <http://dx.doi.org/10.1029/2009JC005997>, 2010.

1292 Milly, P.C.D, et al.: Stationarity is dead: whither water management? *Science* 319:573-574,  
1293 2008.

1294 Mizuta, R.: Intensification of extratropical cyclones associated with the polar jet change in the  
1295 CMIP5 global warming projections. *Geophysical Research Letters*, 39, L19707, 1-6,  
1296 <https://doi.org/10.1029/2012GL053032>, 2012.

1297  
1298 Nakamura, M., and Yamane, S.: Dominant anomaly patterns in the near-surface baroclinicity  
1299 and accompanying anomalies in the atmosphere and oceans. Part I: North Atlantic basin.  
1300 *Journal of Climate*, 22, 880–904. <https://doi.org/10.1175/2010JCLI3017.1>, 2009.

1301

1302 Nakamura, H., Sampe, T., Goto, Ohfuchi, A. W., and Xie, S-P.: On the importance of  
1303 midlatitude oceanic frontal zones for the mean state and dominant variability in the  
1304 tropospheric circulation. *Geophysical Research Letters*, 35, L15709,  
1305 <https://doi.org/10.1029/2008GL034010>, 2008.

1306 Nicholls, R. J., Marinova, N., Lowe, J. A., Brown, S., Vellinga, P., De Gusmao, D., Hinkel, J.,  
1307 and Tol, R. S.: Sea-level rise and its possible impacts given a “beyond 4 C world” in the twenty-  
1308 first century, *Philosophical Transactions of the Royal Society A*, 369, 161–181.  
1309 <https://doi.org/10.1098/rsta.2010.0291>, 2011.

1310 Parey, S.: “Different ways to compute temperature return levels in the climate change context.  
1311 Environmetrics , 21:698–718, 2010.

1312 Philips, M. R., Rees, E. F., and Thomas, T.: winds, sea level and North Atlantic Oscillation  
1313 (NAO) influences: An evaluation; Global Planetary Change, 100, 145-152,  
1314 <http://dx.doi.org/10.1016/j.gloplacha.2012.10.01>, 2013.

1315 Peings, Y., and Magnúsdóttir, G.: Forcing of the wintertime atmospheric circulation by the  
1316 multidecadal fluctuations of the North Atlantic Ocean. Environmental Research Letters, 9  
1317 (2014), 034018, 2014.

1318 Pirazzoli, P.A.: A review of possible eustatic, isostatic and tectonic contributions in eight late-  
1319 Holocene relative sea-level histories from the Mediterranean area. Quaternary Science Review,  
1320 24 (18-19), 1989-2001 , <https://doi.org/10.1016/j.quascirev.2004.06.026>, 2005.

1321 Rosbjerg, R. and Madsen, H.: Design with uncertain design values, Hydrology in a Changing  
1322 Environment”, Wiley, 155–163, 1998.

1323 Pugh, D.J.: Tides, Surges and Mean Sea-Level: A Handbook for Engineers and Scientists. John  
1324 Wiley, Chichester, 472 pp, 1987.

1325

1326 Salas, J.D., and Obeysekera, J.: Revisiting the concepts of return period and risk for  
1327 nonstationary hydrologic extreme events. Journal of Hydrologic Engineering,  
1328 doi:10.1061/(ASCE)HE.1943-5584.0000820, 2013.

1329 Sang, Y.F.: A review on the applications of wavelet transform in hydrology time series  
1330 analysis. Atmospheric Research 122, 8–15. <http://dx.doi.org/10.1016/j.atmosres.2012.11.003>,  
1331 2013.

1332 Sutton, R.S., and Dong, B.: Atlantic Ocean influence on a shift in European climate in the  
1333 1990s. Nature Geosciences, 5, 788–792, 2012.

1334 Seager, R., Harnik, N., Kushnir, Y., Robinson, W., and Miller, J.: Mechanisms of hemispherically  
1335 symmetric climate variability. *Journal of Climate*, 16, 2960–2978, 2003.

1336

1337 Shaw, A.G.P., Tsimplis, M.N.: The 18.6 yr nodal modulation in the tides of Southern European  
1338 Coastal and Continental Shelf Research 30 (2), 138—151,  
1339 <http://dx.doi.org/10.1016/j.csr.2009.10.006>, 2010.

1340

1341

1342 Tyralis, H., Papacharalampous, G., and Tantane, S.: How to explain and predict the shape  
1343 parameter of the generalized extreme value distribution of streamflow extremes using a big  
1344 dataset. *Journal of Hydrology* 574:628–645. doi:10.1016/j.jhydrol.2019.04.070, 2019.

1345

1346 Tomasin A., and Pirazzoli P.A. : Extreme Sea Levels in the English Channel: Calibration of  
1347 the Joint Probability Method. *Journal of Coastal Research* 24 4C 1-13 West Palm Beach,  
1348 Florida July 2008, <https://doi.org/10.2112/07-0826.1>, 2008.

1349 Torrence, C., and Compo, G.P.: A practical guide to wavelet analysis. *B. American*  
1350 *Meteorological Society*, 79, 61–78. [http://dx.doi.org/10.1175/1520-0477\(1998\);](http://dx.doi.org/10.1175/1520-0477(1998);)  
1351 [079<0061:APGTWA>2.0.CO;2](http://dx.doi.org/10.1175/1520-0477(1998);079<0061:APGTWA>2.0.CO;2), 1998.

1352 Trigo, R. M., Osborn, T. J., and Corte-Real, J.: The North Atlantic Oscillation influence on  
1353 Europe: climate impacts and associated physical mechanisms. *Climate Research*, 20, 9–17.  
1354 [10.3354/cr020009](https://doi.org/10.3354/cr020009), 2002.

1355 Trisimplis, M. N., and Josey, S. A.: Forcing of the Mediterranean Sea by atmospheric  
1356 oscillations over the North Atlantic. *Geophysical Research Letters*, 28, 803-806, 2001.

1357 Turki, I., Laignel, B., Kakeh, N., Chevalier, L., and Costa, S., 2015a. Methodology for Filling  
1358 gaps and Forecast in sea level: application to the eastern English Channel and the North

1359 Atlantic Sea (western France), *Ocean Dynamics*, [https://doi.org/ 10.1007/s10236-015-0824-z](https://doi.org/10.1007/s10236-015-0824-z),  
1360 2015a.

1361 Turki, I., Laignel, B., Chevalier, L., Massei, N., and Costa, S.: On the Investigation of the Sea  
1362 Level Variability in Coastal Zones using SWOT Satellite Mission: example of the Eastern  
1363 English Channel (Western France). *IEEE Journal of Selected Topic in Applied Earth*  
1364 *Observations and Remote Sensing*, [http://dx. doi.org/10.1109/JSTARS.2015.2419693](http://dx.doi.org/10.1109/JSTARS.2015.2419693), 2015b.

1365 Turki, I., Massei, N., and Laignel, B.: Linking Sea Level Dynamic and Exceptional Events to  
1366 Large-scale Atmospheric Circulation Variability: Case of Seine Bay, France. *Oceanologia*, 61  
1367 (3), 321-330, <https://doi.org/10.1016/j.oceano.2019.01.003>, 2019.

1368 Turki, I., Massei, N., Laignel, B., and Shafiei, H.: Effects of global climate oscillations in the  
1369 intermonthly to the interannual variability of sea levels along the English Channel Coasts (NW  
1370 France). *Oceanologia* (2020) 000, 1-17, <https://doi.org/10.1016/j.oceano.2020.01.001>, 2020.

1371 Villarini, G., F. Serinaldi, J. A. Smith, and W. F. Krajewski :On the stationarity of annual flood  
1372 peaks in the continental United States during the 20th century, *Water Resources. Research.*,  
1373 45, W08417, doi:10.1029/ 2008WR007645, 2009;

1374

1375 Vousdoukas, M. I., Mentaschi, L., Voukouvalas, E., Verlaan, M., and Feyen, L.: Extreme sea  
1376 levels on the rise along Europe's coasts. *Earth's Future*, 5, 504-323,  
1377 <https://doi.org/10.1002/2016EF000505>, 2017.

1378

1379 Wahl, T., and D. P. Chambers: Climate controls multidecadal variability in U. S. extreme sea  
1380 level records. *Journal of Geophysical Research, Oceans*, 121, 1274-1290,  
1381 doi:10.1002/2015JC011057, 2016.

1382 Wahl, T., and D. P. Chambers: Evidence for multidecadal variability in US extreme sea level  
1383 records. *Journal of Geophysical Research, Oceans*, 120, 1527-1544,  
1384 doi:10.1002/2014JC010443, 2018;

1385 Wong, T. E., Klufas, A., Srikrishnan, V., and Keller, K.: Neglecting model structural  
1386 uncertainty underestimates upper tails of flood hazard. *Environmental Research Letters*, 13,  
1387 074019, <https://doi.org/10.1088/1748-9326/aacb3d>, 2018.

1388 Williams, J., Irazoqui Apecechea, M., Saulter, A., and Horsburgh, K. J.: Radiational tides: their  
1389 double-counting in storm surge forecasts and contribution to the Highest Astronomical Tide,  
1390 *Ocean Sciences.*, 14, 1057-1068, <https://doi.org/10.5194/os-14-1057-2018>, 2018.

1391

1392 Zampieri, M., Scoccimarro, E., and Gualdi, S.: Atlantic influence on spring snowfall over the  
1393 Alps in the past 150 years. *Environmental Research Letters*, 8 (034026), 2013.

1394 Zampieri, M., Toreti, A., Schindler, A., Escoccimarro, E., and Gualdi, S.: Atlantic multi-  
1395 decadal oscillation influence on weather regimes over Europe and the Mediterranean in spring  
1396 and summer. *Global and Planetary Change* 151, 92-100,  
1397 <https://doi.org/10.1016/j.gloplacha.2016.08.014>, 2017.

1398

1399 Zappa, G., Shaffrey, L. C., Hodges, K. I., Sansom, P., and Stephenson, D. B.: A multimodel  
1400 assessment of future projections of North Atlantic and European cyclones in the CMIP5 climate  
1401 models. *Journal of Climate*, 26, 5846-5862, <https://doi.org/10.1175/JCLI-D-12-00573.1>, 2013.

1402 Zhang, R., Delworth, T.L., Sutton, R., Hodson, D.L.R., Dixon, K.W., Held, I.M., Kushnir, Y.,  
1403 Marshall, J., Ming, Y., Msadek, R., Robson, J., Rosati, A.J., Ting, M.F., and Vecchi, G.A.:  
1404 Have aerosols caused the observed Atlantic multidecadal variability? *Journal of Atmospheric*  
1405 *Sciences*, 70, 1135–1144, 2013.

1406